Fouling in membrane bioreactors

Jørgensen, Mads Koustrup

Publication date:
2013

Document Version
Early version, also known as pre-print

Fouling in membrane bioreactors: Effect of cake buildup and compression

Ph.D. dissertation

Fouling i membran bioreaktorer: Effekt af kageopbygning og -komprimering

Ph.D.-afhandling

Mads Koustrup Jørgensen

Department of Biotechnology, Chemistry and Environmental Engineering

Aalborg University

November 2013

Preface

This dissertation is submitted in partial fulfillment of the requirements for obtaining the degree of doctor of philosophy (Ph.D.). The dissertation consists of abstracts in English and Danish, a short thesis, and six supporting papers.

The study was carried out at the Section of Chemistry, Department of Biotechnology, Chemistry and Environmental Engineering at Aalborg University from June 2010 through October 2013. The study was financed in cooperation between Grundfos BioBooster A/S and the strategic research center EcoDesign MBR. A minor part of the study was carried out at University of Colorado, Department of Mechanical Engineering.

I wish to thank my supervisor through the first years of the project, Adjunct Professor Kristian Keiding, for guidance and valuable discussions. Likewise, I would like to thank Associate Professor Morten Lykkegaard Christensen, who was my formal supervisor through the last part of the project, for his helpfulness and cooperation.

Cheers to my fellow Ph.D. students for cooperation and discussions, especially the discussions and cooperation with Thomas Vistisen Bugge. Kim Mørkholt and Lisbeth Wybrandt are acknowledged for their valuable technical help and Grundfos BioBooster A/S for supporting my studies and providing experimental equipment. Furthermore, I owe big thanks to Prof. Alan Greenberg for having me in his laboratory at University of Colorado at Boulder and Ph.D. Elmira Kujundzic for all her help. Finally, I wish to thank Maria for her support and understanding, especially while I was abroad.

Abstract

The growing demand for clean water has led to development of new technologies for wastewater treatment. In this connection, an increasing number of Membrane Bioreactors (MBR) have been installed for wastewater treatment around the World through the last decades. MBR is an alternative to the conventional activated sludge process (CAS), for treatment of municipal and industrial wastewater.

In MBR systems, the membranes are used for separation of the wastewater sludge, integrating the membrane module into a bioreactor, where the sludge components are degraded. The use of membranes for separation has the advantage, compared to the CAS process, where the separation is done by settling, that the effluent (permeate) is less harmful to the local environment where it is led out and can even be reused, e.g. for irrigation purposes. Furthermore, the MBR enables handling of high sludge concentrations, efficient degradation of the sludge and a low footprint compared to the CAS process.

However, the MBR process performance is limited by accumulation of sludge components on the membranes, called membrane fouling. Fouling evolves over filtration time and gives higher hydraulic resistance. The higher hydraulic resistance results in lower production of permeate at constant pressure operation, or requires higher pressure at constant flux operation. This places demands for frequent physical cleaning (relaxation, backwash, enhanced shear) and with time even chemical cleaning to remove foulants and recover permeability.

The objective of this study is to be able to characterize and simulate fouling at different operating conditions in order to determine the fouling propensity at different systems and operating conditions and minimize energy consumption. For this, a procedure for characterization of short term fouling was developed based on a pressure step experimental filtration protocol combined with a simple modeling approach. This modeling approach was based on cake formation and cake compression.

The cake formation was described from a simple mass balance, with a back transport function representing the effect of shear, sludge concentration and other operating conditions on the back transport of foulants from the membrane. From this, the net transport of foulants towards the membranes could be described, to simulate the amount of cake formed over filtration time. The compressibility of the cake layer was described through the pressure dependency of the specific cake resistance. This model showed to simulate filtration data well, and gave output parameters that provided information of the kinetics of cake formation and the cake layers filtration properties under the given conditions of filtration.

Therefore, the model can serve as a tool to characterize the effect of different operating conditions on membrane fouling and thereby filtration performance, which is an important step for reducing operating costs of MBR systems.

It was found, that the cake formation governs the filtration performance during the short term filtration experiments. In the studies of cake formation it was shown, that the enhanced shear by higher rotation of membrane discs gives a higher back transport, and thereby less fouling. Meanwhile, higher sludge concentrations give lower back transport and thereby more fouling. These effects on back transport has been included in another model to describe the effect of shear stress and sludge concentration on back transport, which can be utilized to find optimal operation conditions in terms of amount of permeate produced per amount of energy for creating shear.

The effect of cake layer compressibility was observed through the cake layers resistance response to changes in pressure, with higher resistance at high pressures, and lower resistances at lower pressures. This showed that the kinetics of cake compression was faster than the kinetics for cake formation. It was also found, that the compression of cakes to high extent was reversible. Hence, as pressure on a compressed cake is released it swells back to its original structure.

The last part of the project involved development of a technique for monitoring and characterizing membrane fouling online. A method for on-line and real time detection of sludge fouling during membrane filtration was developed based on ultrasonic reflectometry, as this method can detect fouling on membranes through turbid feed streams. The method was shown to work at diluted sludge samples, and detected denser (more compressed) fouling layers at higher pressures, which confirms the viscoelastic behavior of sludge fouling layers formed on membranes.

Dansk Resume (Danish abstract)

Det stigende behov for rent vand har ført til udvikling af nye teknologier til rensning af spildevand. I den forbindelse er der installeret et stigende antal Membran Bioreaktorer (MBR) globalt gennem de sidste årtier. MBR systemer er en alternativ teknologi til behandling af spildevandslam fra kommunalt og industrielt spildevand.

I MBR systemer sker separationen af slammet ved membranfiltrering, hvor et membranmodul er integreret med en bioreaktor, hvor slammets komponenter nedbrydes. Fordelen ved at bruge membraner til separation i forhold til den konventionelle aktiv slam (CAS) proces hvor separationen af slam sker med bundfældning, er at udløbsvandet (permeatet) er renere. Derfor er udløbsvandet mindre skadeligt for det miljø, hvor det udledes, og kan genbruges til eksempelvis kunstvanding. Derudover er det muligt at operere ved højere slamkoncentrationer ved MBR processen i forhold til CAS processen, hvilket giver en effektiv nedbrydning af slammet, færre omkostninger til slamdeponering og gør processen mindre pladskrævende.

MBR systemernes effektivitet begrænses dog af dannelsen af et lag som blokerer membranerne, kaldet fouling. Foulingen udvikles løbende gennem filtrering og øger den hydrauliske modstand. Ved drift med konstant tryk giver den højere modstand en lavere produktion af permeat, mens ved drift med konstant produktion af permeat, stiger det tryk, der skal til, for at opretholde en konstant produktion af permeat. Dette kræver løbende fysisk rensning og over tid også kemisk rensning af membranerne for at gendanne membranernes permeabilitet.

Formålet med dette Ph.D. projekt har været at udvikle metoder til at karakterisere og simulere fouling ved forskellige driftsparametre og derigennem mindske energiforbruget til drift af MBR anlæg. Til dette blev der udviklet en procedure til karakterisering af fouling i kortidsforsøg baseret på tryk-step forsøg kombineret med en simpel modellering af processen. Denne model var baseret på, at foulingen sker i form af kagedannelse og kagekomprimering.

Kagedannelsen er beskrevet fra en simpel massebalance mellem transporten af slamkomponenter ind mod membranen og tilbagetransporten, beskrevet ved en funktion, som er afhængig af væskestrømning, koncentration og andre driftsparametre. Derved kunne den samlede transport af slamkomponenter ind mod membranen beskrives og derigennem modellere aflejringen af kage på membranen. Kagens kompressibilitet blev beskrevet gennem den specifikke kagemodstands trykafhængighed. Denne model kunne give en god simulering af foulingen observeret i filtreringsdata fra tryk step forsøgene. Tilpasning af modellen til eksperimentelle data gav parametre som beskrev kinetikken i kageopbygning og kagelagets filtreringsegenskaber under de givne filtreringsforhold.

Den udviklede model kan bruges som et redskab til at karakterisere effekten af forskellige driftsindstillinger på fouling og derved filtreringsegenskaberne. Dette er et vigtigt skridt mod at reducere driftsomkostningerne for MBR anlæg.

Forsøg viste, at kagedannelsen styrer filtreringen gennem korttidsforsøg. Ved at øge væskestrømningerne henover membranen ved at øge rotationshastigheden af en roterende membran-disk, opnås en højere tilbagetransport og derved lavere fouling. Højere koncentration giver derimod lavere tilbagetransport og derfor mere kagedannelse. Effekten af væskestrømning og slamkoncentration på tilbagetransporten er blevet beskrevet i en matematisk model. Denne kan bruges til minimering af energiforbruget til filtrering, ved at bestemme de forhold for væskestrømninger og slamkoncentration, hvor energiforbruget relativt per produceret mængde permeat er lavest.

Kagelagets kompressibilitet blev observeret ved en stigning i filtreringsmodstand når trykket blev hævet og et fald i modstanden når trykket blev sænket. Dette viste, at kagekomprimering sker hurtigere end kageopbygning og at komprimeringen i høj grad er reversibel.

I den sidste del af projektet blev der udviklet en metode til detektion og monitorering af fouling on-line, baseret på ultrasonisk reflektometri. Metoden kan detektere forløbet af fouling under filtrering af fortyndede slamprøver og også her blev der vist tegn på, at foulinglaget dannet ved membranfiltrering af slam er kompressibelt.

List of supporting papers

I. Jørgensen, M.K., Bugge, T.V., Christensen, M.L., Keiding, K., 2012. *Modeling approach to determine cake buildup and compression in a high-shear membrane bioreactor*. Journal of Membrane Science 409-410, 335-345.

II. Jørgensen, M.K., Keiding, K., Christensen, M.L., 2013. *On the reversibility of cake buildup and compression in a membrane bioreactor*. Submitted to Journal of Membrane Science.

III. Jørgensen, M.K., Pedersen, M.T., Bentzen, T.R, Christensen, M.L., 2013. *Dependence of shear and concentration on fouling in a membrane bioreactor with rotating membrane discs.* Submitted to AIChE Journal.

IV. Bugge, T.V., Jørgensen, M.K., Christensen, M.L., Keiding, K., 2012. *Modeling Cake Build-up under TMP step filtration in a Membrane Bioreactor: Cake Compressibility is Significant*. Water Research 46, 4330-4338

V. Jørgensen, M.K., Pedersen, M.T., Christensen, M.L., Keiding, K., 2012. *Shear effects on fouling layer compressibility in a high pressure membrane bioreactor*. Conference proceedings, World Filtration Congress, Graz, Austria.

VI. Jørgensen, M.K., Kujundzic, E., Greenberg, A.R., 2013. *Effect of Pressure on Fouling of Microfiltration Membranes by Activated Sludge*. Not submitted.

Table of contents

1. Introduction

Wastewater sludge has been treated with the conventional activated sludge (CAS) process since the start of the 20th century [Meng et al., 2012]. The CAS process consists of biological degradation of organic sludge compounds in a bioreactor. The combination of nitrification and denitrification removes nitrogen while phosphorous is removed by biological and chemical treatment. The separation of sludge into a water phase and a concentrated sludge phase takes place by sludge floc settling in separate settling tanks.

The demand for alternative technologies for wastewater treatment is growing due to enhanced need for efficient wastewater treatment and reuse [Judd, 2011]. One of the drivers behind this need is the pertinent legislation e.g. The Water Framework Directive (European Union) and The Clean Water Act (USA) that sets higher criteria for the quality of water being discharged, in order to prevent pollution of receiving waters. The use of legislation to improve the efficiency and security of water services is only expected to increase with the higher stress on water resources in the future. Water stress occurs, when the demand for water exceeds the amount of water. In 1990 1.8 billion people lived in water stressed countries, while in 2025, 5.1 billion people are expected to live in water stressed countries. The higher criteria for quality of water discharged to receiving waters and the higher demand for water recycling has promoted the implementation of membrane bioreactors (MBR). Between 2008 and 2013 more than 2500 MBR installations have been in operation worldwide with an annual growth rate of 10.5 % [Meng et al., 2012]. MBR installations for municipal wastewater treatment account for roughly 75 % of the installed MBR plants [Lesjean and Huisjes, 2008; Drews, 2010; Judd, 2011].

In the past decades the MBR has been studied intensively as an alternative to the CAS process [Drews, 2010; Judd, 2011; Meng et al., 2012]. MBR combines the microbial degradation with the sludge dewatering process by integrating a membrane in the bioreactor, either with an immersed or sidestream membrane configuration as illustrated in Figure 1.1.

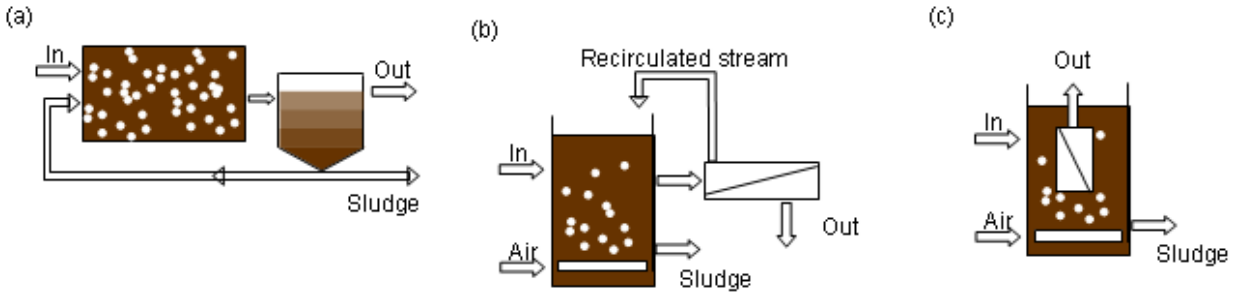

Figure 1.1: Illustration of the CAS process (a), the sidestream MBR (b) and the immersed MBR (c).

The sidestream MBR was the first MBR system, developed in 1968. Sidestreams MBRs typically works with pressures up to 0.5 bar. However, it was limited by high energy consumption for pumping sludge in the sidestream module [Meng et al., 2012]. The turning point came when Yamamoto et al. (1989) introduced the immersed membrane MBR. Here, no energy is required for pumping sludge through a filtration module, as immersed membranes are scoured by air bubbles, which also aerate the sludge. In the immersed MBR systems, the pressure is often in a range of 0.01-0.08 bar generated by a vacuum at the permeate side of the membrane [Ho and Zydney, 2006; Meng et al., 2012].

The MBR has a number of advantages compared to the CAS for wastewater treatment. The ultra- and microfiltration membranes used in MBR systems retain sludge components larger than the membrane pore size [Drews et al., 2010; Meng et al., 2012]. Hence by applying membranes with pores smaller than 500 nm, single cell bacteria and sludge flocs will be retained and the permeate effluent of the MBR system will only contain components smaller than this particle size. Compared to the CAS process this gives a much cleaner effluent that does not contain any bacteria.

The use of membranes for separation allows for higher sludge concentrations (typically 8-18 g/L, [Drews, 2010]) than used in CAS processes (typically up to 5 g/L [Ho and Zydney, 2006]), where the concentration may not be too high, as this will limit the settling. Using high sludge concentrations gives lower production of excess sludge, which reduces the costs for sludge disposal by up to a factor of three. Operation at high sludge concentrations is also associated with lower costs for sludge disposal, efficient degradation of organic compounds, i.e. biological oxygen demand (BOD) and chemical oxygen demand (COD) [Ho and Zydney, 2006; Meng et al., 2009]. The high solid retention time (SRT) at high sludge concentrations promotes growth of slowly growing microorganisms degrading specific organic pollutants [Le-Clech, 2010]. Furthermore, the high sludge concentration gives a lower volume of the bioreactor. Combined with the un-necessity of a settling tank, the MBR system has a much lower footprint than the CAS system. The mentioned advantages have made the MBR technology competitive to CAS processes and state-of-the-art in wastewater treatment.

However, the widespread of the technology is still limited by membrane fouling. Membrane fouling occurs as sludge components deposit on or adhere to the membrane. This gives a higher hydraulic resistance of the membrane, requiring higher transmembrane pressure (TMP) to produce the same flow of permeate or gives lower permeate flux over time in constant pressure operation. Hence, membrane fouling enhances the operating expenses due to higher energy consumption and less production of water. Up to 70% of the energy consumption of operation of MBR plants is related to membrane fouling, and the flux of water through the membranes is only 10-30% of that through clean membranes [Böhm et al., 2012]. Furthermore, over time an irreversible layer of

fouling develops, which places demand for chemical cleaning or eventually replacement of the membranes [Drews, 2010].

Therefore, by limiting membrane fouling and the expenses related to that, the productivity and widespread of MBR systems can be increased. To do so, an in-depth understanding of fouling mechanisms is required.

2. Fouling in Membrane Bioreactors

The permeate flux through a membrane, J, is a function of TMP, filtrate dynamic viscosity, μ, and resistance of the membrane, R_m, according to the Darcy equation:

$$J = \frac{TMP}{\mu(R_m + R_f)} \quad (2.1)$$

During filtration of suspensions and solutions, e.g. MBR sludge, the suspensions components accumulate at the membrane surface creating a fouling layer. This layer contributes with an additional resistance to filtration, R_f. Hence, during filtration at constant TMP, the flux will decline with time as R_f increases, while at constant flux filtration TMP increases with time [Meng et al., 2009; Drews, 2010]. Over time in constant flux filtration, where the TMP rises gradually as the membrane is fouled, the TMP suddenly jumps due to intensification of the fouling, denoted the "TMP-jump".

To recover permeability, the fouling layer is periodically removed either with relaxation or backwash [Judd, 2011]. For relaxation, there is a break in filtration, i.e. TMP = 0), hence there is no drag of foulants towards the membrane, but only removal of foulants by shear. During backwash the constituents of the layer is transported away from the membrane by flow reversal through the membrane induced by a negative TMP. Furthermore, enhanced shear is used to prevent fouling. In immersed MBRs this is typically done by air scouring of the membranes, while in sidestream MBRs it is achieved via high crossflow over the membrane.

The fouling can be divided into removable, irremovable and irreversible fouling [Meng et al., 2009; Drews, 2010; Judd, 2011], where the removable fouling is removed by the physical cleaning protocol, while the irremovable fouling has to be removed by chemical cleaning of the membranes. Finally, some of the fouling is irreversible and places demands for membrane replacement. The reversible fouling occurs over shorter time frames than irremovable and irreversible fouling [Drews, 2010].

In MBR sludge the components that can foul the membrane are sludge flocs, single cell bacteria, colloids, organic macromolecules and salts [Meng et al., 2009; Drews, 2010].

2.1 Fouling mechanisms

The components of the sludge can form fouling layers by the following mechanisms [Drews, 2010]:

- Cake formation. Reversible fouling that can be removed by e.g. relaxation [Bae and Tak, 2005; Wang and Wu, 2009]

- Pore blocking and adsorption. Partly irremovable/irreversible fouling, which can be removed using backwash or chemical cleaning [Bae and Tak, 2005; Drews, 2010]
- Gel layer and biofilm formation. Irremovable/irreversible fouling [Lee et al., 2008; Wu and Fane, 2012]
- Scaling. Irremovable/irreversible fouling, which can only be removed by chemical cleaning [Ognier et al., 2002]

Of these mechanisms, the cake formation and gel layer formation has been given most attention in literature on MBR fouling. During filtration concentration is polarized by macromolecules as the concentration near the membrane reaches the gel point. At this concentration is the gel layer is formed. The gel layer is described as irremovable/irreversible fouling [Meng et al., 2009] and has a higher specific cake resistance and lower porosity than the cake layer [Wang et al., 2012].

By taking account of the listed fouling mechanisms, the fouling resistance, R_f, can be calculated from the following expression:

$$R_f = R_c + R_p + R_g + R_s \tag{2.2}$$

where R_c is the cake resistance, R_p is resistance from pore blocking, R_g is resistance from the gel layer, while R_s is the resistance from scaling.

Jiang et al. (2003) has shown that when starting filtration on a clean membrane, the pore blocking leads to an instant increment in resistance, but only during the first few seconds of filtration. After this, the more dominant cake formation takes over and increases over time. This layer has been shown to be reversible, and is removed by physical cleaning and controlled by shear. Although cake formation has shown to give higher filtration resistance and lower process performance, a study by Giraldo and LeChevallier (2007) shows that the cake can actually be beneficial for the operation of MBRs, as it serves as a protective layer for the membrane, limiting irreversible pore blocking. Therefore, forming a thin cake layer with a low resistance can improve MBR performance by limiting irreversible fouling.

The formation of a loose cake structure and a dense gel layer close to the membrane is illustrated in Figure 2.1.

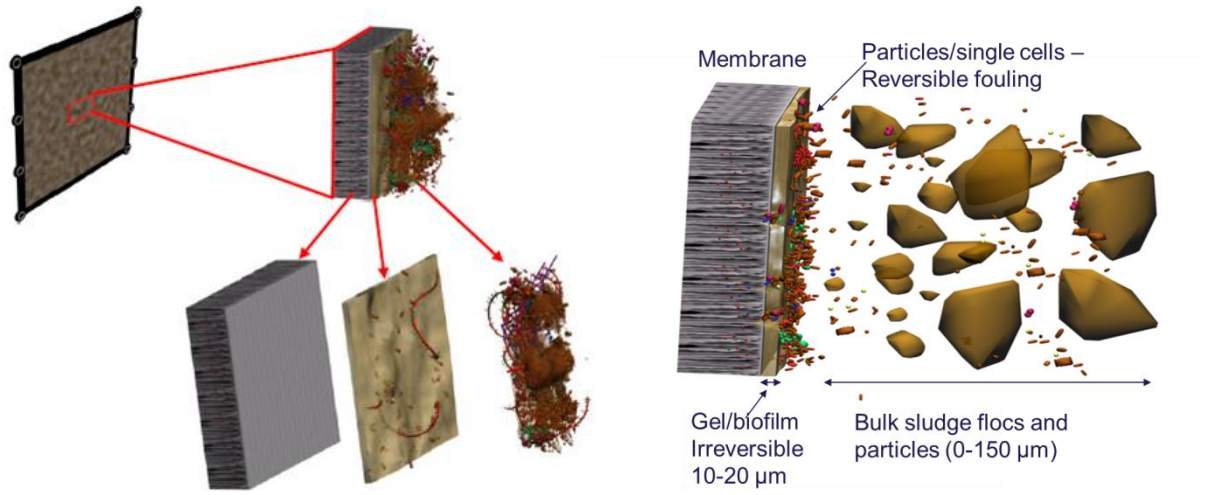

Figure 2.1: Illustration of a fouled membrane with a hydraulic resistance consisting of the clean membrane resistance, resistance of the dense gel layer and the loose cake structure. Larsen et al. (2013)

In several studies it is found that the main contributor to MBR fouling is sludge cake formation [Meng et al., 2009; Wang and Wu, 2009]. The cake forms at supercritical flux operations, hence the drag of foulants has to be high enough to form a cake layer deposit. However, at sub critical constant flux operation, cake formation occurs in two steps [Ognier et al., 2004]; in the first step the flux is too low to form a cake and instead a gel layer forms. In the second step, the resistance formed locally on the membrane gives a higher flux through non-covered parts of the membrane where the critical flux is exceeded, thus cake formation starts.

R_c can be calculated from the following equation [Wang and Wu, 2009].

$$R_c = \alpha \cdot \omega_c \qquad (2.3)$$

α is the specific cake resistance, representing the characteristics of the sludge and the cake layer, and ω_c is the amount of cake.

During cake layer formation the development in amount of cake gives a linearly increasing cake resistance over time [Ho and Zydney, 2006; Wang and Wu, 2009]. The linearity between resistance and amount of deposited materials is not observed for e.g. pore blocking [Ho and Zydney, 2006].

The specific cake resistance has shown to depend on operational parameters such as shear and pressure. From other membrane filtration systems, it is well established, that the cake layer formed on the membrane is compressible, hence increasing pressure increases the specific cake resistance [Sørensen and Sørensen, 1997a; Christensen et al., 2009]. For MBR systems, some studies have described the compressibility of the sludge cake layer on the membrane to have influence on the filtration. In Teychene et al. (2011) it is found that the filtration

process can be optimized by modifying the compressibility of the fouling layers in MBR supernatant filtration with fine particle addition. Compressibility effects are also observed in Zhang et al. (2006) where the TMP jump at constant flux filtration is ascribed to sudden changes in cake structure with the higher levels of TMP.

Therefore, the linearity between the cake resistance and amount of cake is only observed during constant pressure filtration, where the specific cake resistance is constant.

2.2 Fouling parameters

The basic physical-chemical terms for formation of fouling layers is described with the mass balance in Eq. 2.4 and covers a variety of parameters influencing on the development of fouling [Bacchin et al., 2006; Le-Clech et al., 2006].

$$\frac{d\omega}{dt} = J \cdot \phi - D_B \frac{d\phi}{dx} + p(\zeta) + q(\tau) \qquad (2.4)$$

The permeation drag is represented by the sum of the flux, J, and the volume fraction of the foulants, ϕ, which is proportional to the total suspended solids concentration (TSS). The Brownian diffusion, which affects mainly the smaller sludge compounds such as colloids and macromolecules, is expressed through the Brownian diffusion coefficient, D_B, and the gradient of foulant volume fraction from the membrane, $d\phi/dx$. The foulant-foulant and foulant-membrane electrostatic interaction, which occurs in adsorption, is described through $p(\zeta)$. The shear effect on deposition is expressed through $q(\tau)$ which affects the larger compounds such as sludge flocs and large colloids.

Enhancing shear by increasing crossflow velocity or air scouring of the immersed membrane increases back transport of foulants and lowers fouling. In contrast to Brownian diffusion, the higher foulant particle sizes give higher back transport promoted by shear. The effect of particle size on diffusion coefficients for Brownian diffusion, D_B, can be described from the Stoke-Einstein equation, Eq. 2.5a, while the shear induced diffusion coefficient, D_S, can be described from a relationship proposed by Leighton and Acrivos (1987), Eq. 2.5b.

$$D_B = \frac{k_B T}{3\pi\mu d_p} \qquad (2.5a)$$

$$D_S = 0.5\left(\phi \frac{d_p}{2}\right)^2 \frac{\tau}{\mu} \qquad (2.5b)$$

In Eq. 2.5a and Eq. 2.5b, k_B is Boltzmann constant, T is the temperature, d_p denotes the diameter of particles, ϕ is the volume fraction of particles in the suspension (valid up to 0.2) and τ is the shear stress. Assuming a viscosity

of $1.09 \cdot 10^{-3}$ Pa·s and using a shear stress of 1 Pa, a sludge concentration of 10 g/L corresponding to a particle volume fraction of 0.0096, and a temperature of 20 ºC, the diffusion coefficients for Brownian and shear induced diffusion can be calculated as a function of particle size. This is done in Figure 2.2.

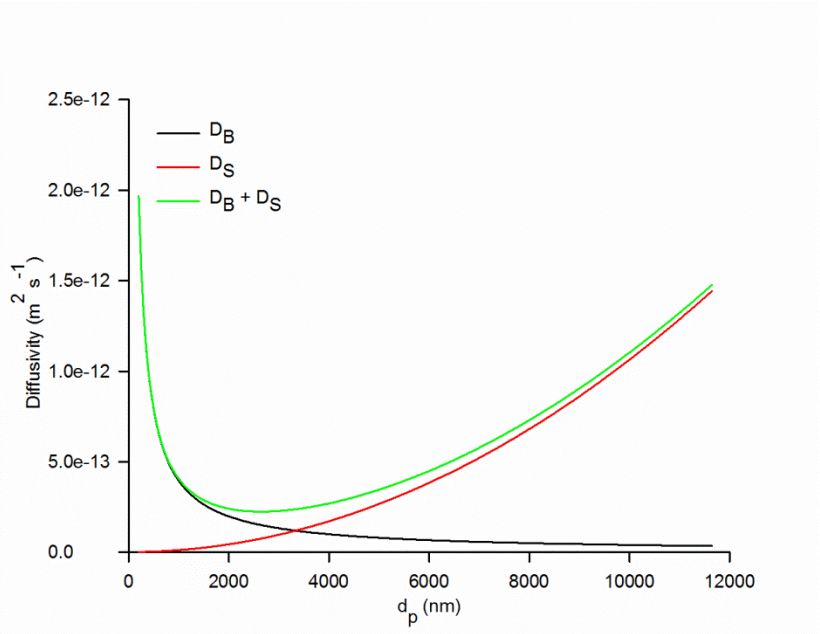

Figure 2.2: Diffusivity for Brownian diffusion (D_B), shear induced diffusion (D_S) and a combined diffusivity ($D_B + D_S$) as function of particle diameter for 10 g/L suspension at a shear stress of 1 Pa.

It is observed, that with lower particle size, the higher is the Brownian diffusion, while with higher particle sizes, the shear induced diffusion increases. At a particle diameter above 3-4 μm the shear induced diffusion is the dominant mechanism for back transport of foulants. However, the transition between Brownian diffusion and shear induced diffusion as the dominant back transport mechanism depends on shear stress; increasing shear stress enhances D_S which reduces the particle diameter where the transition occurs. It can be concluded from Figure 2.2, that there is an intermediate range of particle sizes (0.5 – 5 μm) that are not effectively transported away from the membrane, whereas larger particles are transported away from the membrane by shear induced diffusion and smaller particles (colloids) are transported away from the membrane by shear induced diffusion.

Smaller particles form more compact fouling layers with a higher resistance, than larger particles [Wisniewski and Grasmick, 1998]. Besides from the particle size, the particle size distribution influences the fouling layer morphology, as a broader distribution will enable smaller particles to blind the cavities formed by the larger particles [Lim and Bai, 2003].

In some studies it is found that shear can give sludge deflocculation with release of soluble microbial products (SMP) and therefore give lower filtration properties of the sludge [Stricot et al., 2010]. The nature of the sludge flocs is important to the sludge filtration characteristics and is affected by the ratio of polyvalent ions to monovalent ions [Van den Broeck et al., 2010]. Increasing the concentration of polyvalent ions gives flocculation with larger flocs that forms a secondary membrane, protecting the membrane from soluble substances. On the other hand increasing the concentration of monovalent ions gives sludge deflocculation and thereby deteriorates filtration properties.

Generally, increasing suspension concentration intensifies fouling, but the influence of concentration has been shown to be more complex for MBR systems [Loussada-Ferreira et al., 2010]. The $p(\zeta)$ term in Eq. 2.4 covers the membrane physical chemical characteristics compared to the foulants interaction, and is therefore a function of various parameters such as sludge characteristics, concentration of extracellular polymeric substances (EPS), membrane morphology, material, and particle-particle interaction. It is this term that through e.g. particle-particle or particle-membrane interaction gives irreversible fouling, but can also represent repulsion increases back diffusion.

Due to the obvious complexity of the interaction between a complex sludge mixture and membrane filtration module phenomenological studies of single parameters influence on fouling are often limited by the interaction between parameters and variances in characteristics from plant to plant. Instead, methods have been developed to study the fouling propensity of different types of sludge in individual systems at varying operation conditions.

2.3 Characterization of fouling

Several approaches have been developed to monitor or characterize fouling in MBRs. Monclus et al. (2011) developed a method to online monitor the evolution of fouling by the slope of the TMP over time required to maintain a constant flux. As fouling develops, the slope will increase, and prior to the TMP-jump the slope will increase with a rate exceeding the limits of sustainable operation. By monitoring this, operators will know when to perform membrane cleaning or change operational conditions to mitigate fouling.

To characterize fouling propensity of sludge in MBR plants over time, some filtration characterization methods have been developed with the Delft filtration characterization method (DFCm) Berlin Filtration Method (BFM) and the VITO Fouling Measurement method (MBR-VFM) being the most used methods [De la Torre et al., 2009; Drews, 2010].

In DFCm a sidestream ultrafiltration membrane filtrates sludge from a bioreactor with a crossflow velocity of 1 m/s and a constant flux of 80 $L \cdot m^{-2} \cdot h^{-1}$ (LMH) until 20 L of permeate has been collected. From the increase in

resistance, the increment in resistance is calculated, which is proportional to the fouling propensity. The shear generated by the high crossflow velocity is not comparable to the shear working on an immersed membrane surface, but the method shows the fouling propensity of sludge, which is a measure of filtration properties.

The BFM and MBR-VFM methods use immersed membranes for sludge filtration, flatsheet and tubular membranes, respectively [Huyskens et al., 2008; De La Torre et al., 2010]. At constant flux operations, the filterability of the sludge is assessed through the increment in TMP found from flux stepping experiments.

2.3.1 Flux- and TMP stepping

Flux- and TMP stepping is widely used to determine the fouling propensity of filtrations system under varying operational conditions [Le-Clech et al., 2003].

In flux stepping the flux is stepped between different constant values, to measure the development in TMP at conditions above and under critical conditions. In TMP step experiments, the development in flux is measured while TMP is stepped. In the classical protocol, TMP is stepwise increased until a maximum level is reached, where after TMP is stepped down again. In a protocol proposed by van der Marel et al. (2009), intermittent relaxation steps are applied between each step, in order to remove fouling accumulated during the individual step. With this approach the reversibility of fouling can be studied. Furthermore, pre-step and post-step protocols can be used. With these, a low reference level of flux or TMP is applied between the intermittent TMP steps [Le-Clech et al., 2003]. An example of a post-level TMP step experiment is shown in Figure 2.3.

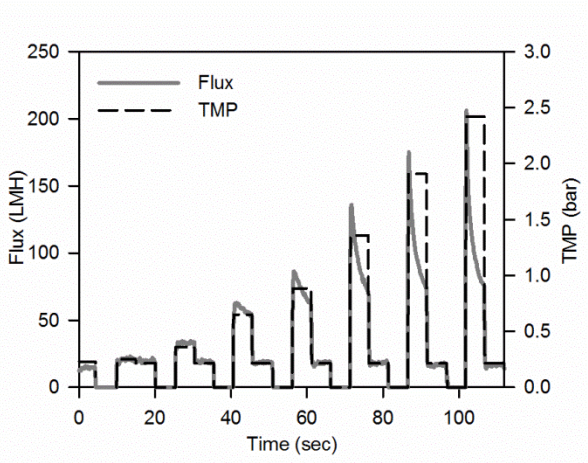

Figure 2.3. Development in flux and pressure over time in a TMP step experiment. From Paper I.

The TMP step experiments show higher flux decline at higher TMP, in accordance with Eq. 2.4. From the post-reference level of TMP, the permeability of the membrane and fouling layer. After the relaxation phase the flux

is in some studies observed to be restored [Paper I; van der Marel et al., 2009], which shows that the fouling layer is reversible. This implies that the fouling layer consists of a reversible cake layer.

2.3.2 Critical and limiting flux

The Flux- and TMP step experiments are usually analyzed with the critical flux concept. With the critical flux concept, fouling can be characterized in various systems with complex fouling mechanisms with a critical or limiting flux presenting the fouling propensity of the given system or sludge.

The critical flux, J_{crit}, was defined by Field et al. (1995) as "the flux below which a decline in flux does not occur; above it fouling is observed". Hence, the critical flux is the flux level at which deposition on the membrane, induced by permeation, starts. The critical flux is divided into a strong and weak form.

The strong form critical flux is where the relationship between flux and TMP deviates from the water *J-TMP* relationship, which is a straight line depending on the membrane resistance [Bacchin et al., 2006]. In the weak form of critical flux, there is still a linear relationship between flux and TMP in the lower range, but it is lower than that of water, due to almost instantaneous loss of permeability caused by adsorption, pore blocking or concentration polarization. Still, the weak form of critical flux is found from the flux level above which the flux no longer increases linearly with TMP (Fig. 1) [Bacchin et al., 2006]. For MBR fouling, the critical flux is observed in the weak form, as adsorption cannot be ruled out even without permeation.

Equivalently, a critical flux for irreversible fouling, $J_{c,i}$, has been introduced [Bacchin et al., 2006; van der Marel et al., 2009]. $J_{c,i}$ is defined as the flux above where irreversible fouling occurs and can also be determined from stepping experiments. Plotting the initial flux and initial TMP of each step after a cleaning step as in Figure 2.4 gives a straight line relationship until the critical flux for irreversible fouling is reached [Espinasse et al., 2002; Rayess et al., 2011]. However, the irreversibility found with this method is limited to the specific physical cleaning protocol.

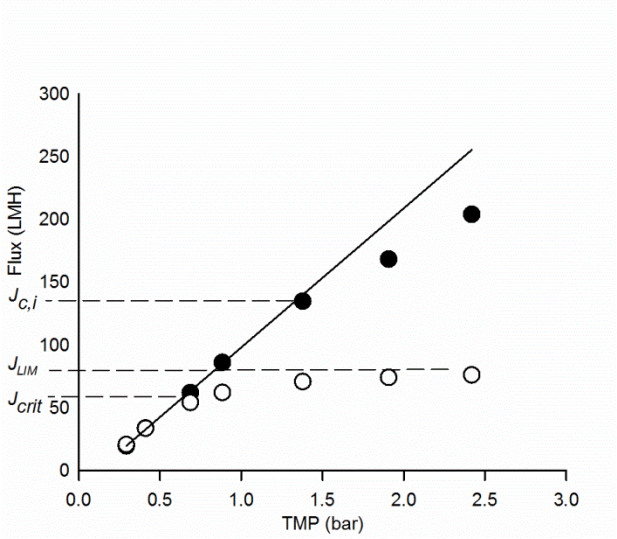

Figure 2.4: Initial (○) and steady state (●) flux vs. TMP from a TMP step experiment

From Figure 2.4 it is observed, that the steady state flux vs. TMP levels of at high TMPs. Hence, at a high steady state flux increasing pressure does not have any influence. At this level, the pressure independent steady state flux has been reached, also denoted the limiting flux [Bacchin et al., 2006]. At this level, the back transport of foulants from the membrane equals the permeation drag. Hence from Eq. 2.4 there is no further deposition of foulants. The limiting flux relates directly to the mass balance in Eq. 2.4. The critical flux, on the other hand, relates to the mass balance in that when the relationship between permeation drag and back transport is sufficiently high, a critical deposit formation on the membrane is reached. Therefore, changes in operation conditions such as shear or sludge characteristics will be reflected by the critical and limiting flux.

Related to the critical flux the term sustainable flux has been introduced, which distinguishes between flues at high or low (sustainable) fouling rates [Bacchin et al., 2006]. However, the criterion for a sustainable fouling rate has to be defined for each individual application.

2.3.3 Modeling

As described in section *2.2 Fouling parameters*, the complexity of sludge fouling makes it possible to only make qualitative guidelines for specific operational parameters or sludge properties with respect to fouling mitigation. However, through modeling approaches it may be possible to understand the fundamental fouling mechanisms of specific sludges in specific systems.

Modeling fouling in membrane bioreactors have focused on the development in amount of cake described with a mass balance as in Eq. 2.4 [Ho and Zydney, 2006]. The effect of cake buildup, hence development in amount of

cake, ω_c, is incorporated into Eq. 2.3 to calculate the cake resistance over time, to be able to calculate the development in flux over time. However, only in two studies a dynamical model has been used for membrane bioreactor fouling, incorporating the influence on pressure on the specific cake resistance [Giraldo and LeChevallier, 2006; Li and Wang, 2006], although the effect of compressibility has shown to be highly relevant in other studies of membrane fouling.

3. Objective

The aim of this Ph.D. project is to establish knowledge on cake layer formation on membranes in membrane bioreactors.

Until now, many studies have focused on finding the influence of different parameters, such as shear, concentration, etc., on formation of fouling. Since these parameters influence are linked to the specific sludge or system studied, this study will focus on developing simple and systematic experimental approaches to study the effect of different operational parameters on fouling, based on TMP step experiments. Furthermore, a systematic study of the influence of cake compression will be investigated by use of TMP step experiments.

Data from the TMP step experiments will be studied systematically by a modeling approach, describing the short term fouling as a consequence of cake formation and cake compression. The output of these is model parameters describing the buildup and compressibility of cakes that depends on operational conditions. This is done with emphasis on developing a method to characterize fouling and use this to optimize filtration performance in real MBR systems.

Finally, it will be explored if new monitoring techniques can provide deeper knowledge on the formation of fouling layers through direct observation of the formation and behavior of fouling layers during MBR filtration.

In Chapter 4 the chosen experimental systems and approach for studying fouling will be presented. After this, the cake buildup at different operational conditions in MBR will be described, followed by a chapter describing cake compressibility. After this, a modeling approach based on cake buildup and compression is presented. Here, the perspectives of the model for characterizing fouling mechanisms and as a tool to show how to control filtration processes at different operational and sludge conditions are discussed with emphasis on improving performance of MBRs. Finally, it will be shown, how online monitoring has the possibility of giving a qualitative and quantitative characterization of fouling on-line in MBR filtration.

4. Membrane bioreactors for studies of fouling

MBR sludge

Sludge from a lab scale MBR and a pilot scale MBR has been used for studies of fouling by TMP step experiments. The lab scale MBR had a volume of 350 L seeded with activated sludge from a local wastewater treatment plant (WWTP). The bioreactor was operated continuously with a synthetic wastewater as a feed. The synthetic substrate consisted of a blend of dog food and fish meal, to obtain chemical characteristics similar to those of wastewater. The substrate had a COD content of 20 g/L and a BOD content of 12 g/L and protein and carbohydrate concentrations of 7 and 5 g/L, respectively. The sludge was fed with a feed-to-microorganism (F:M) ratio of 0.1 mgCOD/mgMLSS/d. The bioreactor had been running for several months to develop sludge with constant chemical characteristics. This was done by keeping the concentration constant around 10 g/L and a solid retention time (SRT) of around 35 days. The MBR had flat sheet membranes with an area of 2 m^2 installed, that were scoured with air (20 L/min/m^2).

The pilot scale MBR consisted of a 1.6-m^3 DN tank, a 1.8-m^3 closed hydrolysis tank, and a 1.8-m^3 N tank with 40 m^2 flat sheet polymeric membranes. The pilot plant was started up with conventional activated sludge from the Aalborg Vest Wastewater Treatment Plant, and had reached stable operating conditions at the time of the experiment.

Filtration units

Three different filtration units for MBR filtration studies have been used; the lab scale MBR with flat sheet membranes, a transportable membrane module for submersion in sludge and a sidestream filtration unit with rotating ceramic membrane discs. The setups of these systems are illustrated in Figure 4.1.

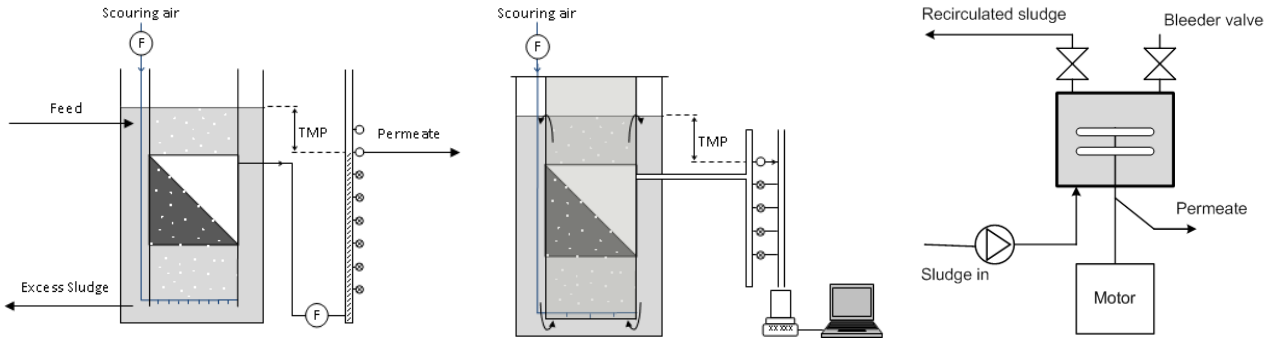

Figure 4.1: A membrane bioreactor with flat sheet immersed membranes (left), a mobile flat sheet filtration module (middle) and a sidestream filtration unit with rotating ceramic discs for filtration of sludge from the lab scale MBR (right).

TMP step experiments on flat sheet membranes on the lab scale sludge were carried out in a separate 175 L tank with an immersed membrane module Fig. 4.1 (left). TMP could be controlled by the difference in water level between the bioreactor and the permeate buffer system, and could be adjusted to eight different levels by the eight different permeate valves, see Figure 4.1. The pressure range of this system was from 0.05 bar to 0.4 bar.

For filtrations on pilot scale sludge with flat sheet membranes, a mobile filtration unit was used with 0.45 m^2 membrane was immersed into a 120 L tank with sludge, aerated with 2.5 L/min for air scouring. The pressure was regulated with a permeate valve system giving TMP in the range of 0.03-0.14 bar.

The sidestream filtration unit was chosen to study MBR fouling for two reasons. First, the studies were carried out in cooperation with Grundfos BioBooster that develops and manufactures MBR systems with rotating ceramic membranes. This was done in order to optimize and characterize the filtration process. Second, a system with rotating membrane discs are useful to study the development of fouling layers at different operational conditions, as the shear on the membrane can be changed by changing the rotation speed. The sidestream filtration unit was connected to the lab scale MBR to do filtrations on the same sludge that was used for flat sheet membrane filtration. A pump, pumping in sludge to the filtration module, adjusted the TMP in a range of 0.3 – 2.5 bar. A motor connected to two ceramic membrane discs (total membrane area of 0.28 m^2) could give rotation speeds in a range of 61 – 360 rotations per minute (rpm). In the Grundfos BioBooster MBR system the pressure range is typically 0.8-1.2 bar and rotation speeds 100-180 rpm.

Design of stepping experiments

Two different TMP step protocols have been used to study the cake formation and cake compression in the membrane bioreactors. These are shown in Figure 4.2.

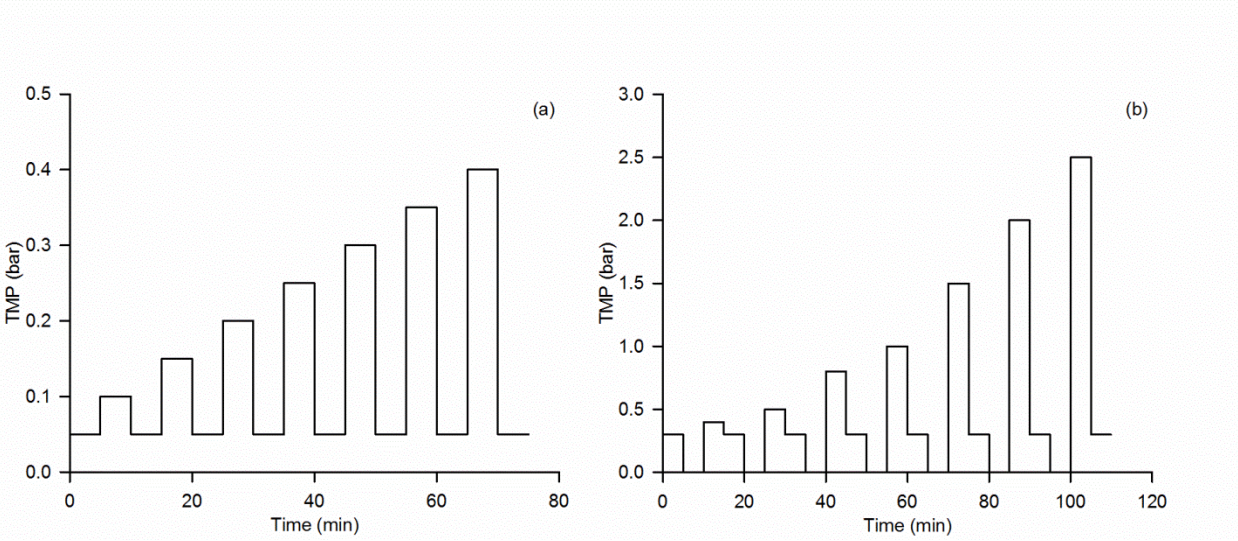

Figure 4.2: Procedure for TMP step experiments used for hollow sheet immersed membrane MBR system in Paper IV (a) and sidestream membrane discs in Paper I (b).

The TMP step protocol for the experiments on the hollow sheet membrane was inspired by van der Marel et al. (2009). At higher pressures, the flux decline will be more and more severe due to operations at supra-critical fluxes. A low pressure step of 0.3 bar was applied before each intermittent TMP step in order to find the permeability and development in flux at sub-critical flux conditions. This protocol was used on sludge from the lab scale MBR in Paper IV.

For TMP steps on the rotating membrane discs filtrating sludge from the lab scale MBR in Paper I, a procedure was developed combining reference steps at 0.3 bar TMP and total relaxation steps. The reference levels showed the permeability and development in flux at sub-critical conditions while the relaxation step was introduced to restore the flux, in order to show the reversibility of fouling at each step. The same procedure was applied for filtration of pilot scale MBR sludge with the rotating membrane disc filtration module in Paper II. In Paper V, the same procedure was used for filtration of lab scale MBR sludge, but without the relaxation steps. This was done in order to study the compression of the cake when increasing pressure from the low reference TMP of 0.3 bar.

5. Cake buildup

5.1 Mass balance for cake formation

For cake formation in crossflow filtration, Figure 5.1 describes the one dimensional transport of foulants towards the membrane [Zydney and Colton, 1986; Davis and Sherwood, 1990; Lee and Clark, 1997].

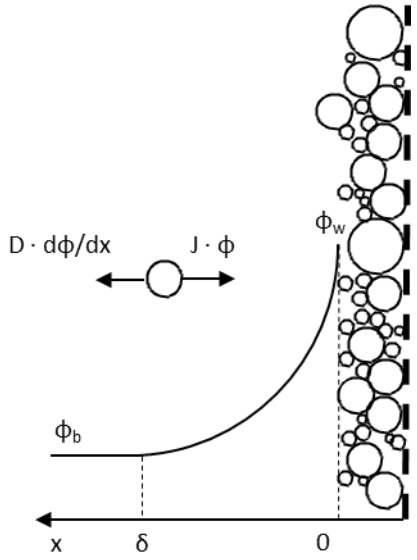

Figure 5.1: Permeation drag, $J \cdot \phi$, and back diffusion, $D \cdot d\phi/dx$, of a foulant near a membrane.

$J \cdot \phi$ represents the permeation drag forming the fouling layer where J is the permeate flux and ϕ is the volume fraction of particles (foulants), proportional to TSS in accordance with Eq. 2.4. The back transport is described as a diffusion phenomenon. The back diffusion of particles occurs as there is a concentration gradient, $d\phi/dx$, created by the foulants accumulated by permeation. The thickness of the boundary layer, δ, is the distance from the high wall volume fraction to the steady bulk volume fraction, ϕ_b. Near the membrane surface the volume fraction of foulants has been reported for different suspensions to reach a maximum value of $\phi_{w,max}$ = 0.58-0.62 [Davis and Sherwood, 1990]. When the volume fraction of particles at the surface of the membrane reaches this value, a stagnant cake has formed. Therefore, as the cake layer has formed, the concentration gradient depends only on the bulk volume fraction. The concentration gradient gives a net diffusion away from the membrane towards the lower bulk concentration with an apparent diffusion coefficient D. The apparent diffusion coefficient accounts for various diffusion mechanisms, such as Brownian diffusion, D_B, and shear induced diffusion, D_S [Huismann et al., 1999].

For steady state in cake buildup, hence $d\omega_c/dt = 0$, the flux remains constant at the flux corresponding to the back transport, J_{BT}. At steady state conditions and if fouling is reversible, the mass balance illustrated in Figure 5.1 can be solved to give the following equation [Lee and Clark, 1997]:

$$J_{BT}\phi = D\frac{d\phi}{dx} = (D_S + D_B)\frac{d\phi}{dx} \tag{5.1}$$

Hence, the back transport flux can be used to describe the mass balance for the development of cake layers, presented in Eq. 5.2 [Lee and Clark, 1997; Ho and Zydney, 2006]:

$$\frac{d\omega_c}{dt} = J\phi - (D_S + D_B)\frac{d\phi}{dx} = (J - J_{BT})\phi \tag{5.2}$$

In Paper I it is argued that the back transport flux, where there is equilibrium between permeation drag and back transport ($d\omega_c/dt = 0$), is similar to J_{LIM}, if a stagnant cake has formed. Hence, in this case, $J_{BT} = J_{LIM}$. However, if a stagnant cake has not formed, the back transport increases with the amount of deposited material, as explained in the following.

During filtration, foulants accumulate over time to create a higher and higher concentration on the membrane or higher amount of deposited material on the membrane, ω. As this concentration increases, the concentration gradient increases, which will enhance back transport. The back transport increases with ω until a stagnant cake has formed. Above this, the concentration gradient and back transport has reached a maximum value, as the concentration corresponding to when a stagnant cake has formed corresponds to $\phi_{w,max}$, explained from Figure 5.1. The back transport dependency of amount of deposited material has been proposed in Paper I and Paper IV to have the following form:

$$J_{BT} = J_{LIM}\left(1 - e^{-\frac{\omega}{\omega_{crit}}}\right) \tag{5.3}$$

where ω_{crit} is the critical amount of deposit. In Figure 5.2, Eq. 5.3 is plotted.

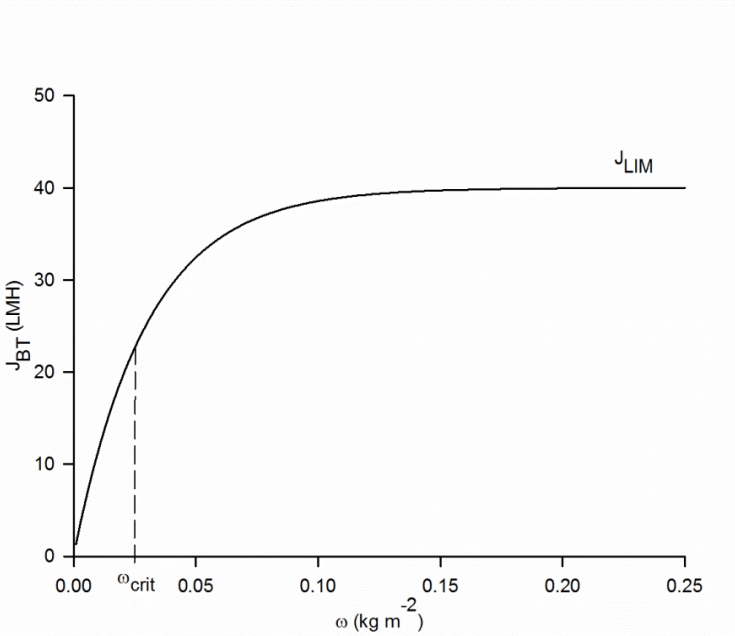

Figure 5.2: Dependency of amount of membrane deposit on the back transport of foulants.

The figure shows an increasing back transport with increasing ω. As ω reaches ω_{crit} the increment of J_{BT} is less significant with ω until J_{BT} levels off at a value corresponding to J_{LIM}.

From the mass balance, it can be inferred that the level of the flux at a given time compared to the limiting flux controls the development of fouling layers in the following way:

- If $J > J_{LIM}$ then $0 < d\omega_c/dt$, i.e. the stagnant cake layer is growing and the flux declines
- If $J = J_{LIM}$ then $d\omega_c/dt = 0$, i.e. the amount of cake is steady and so is flux.
- If $J < J_{LIM}$ then $d\omega_c/dt < 0$, i.e. no cake layer is developed, and if any present it is removed, which gives restoration of permeability.

Hence, when a cake has developed on the membrane, it is the cake properties and the limiting flux that controls the filtration. This is exemplified by TMP-step experiments on 10 g/L lab scale MBR sludge with a sidestream filtration module with rotating ceramic discs average pore sizes of 60nm and 200 nm respectively. The results of this are presented in Figure 5.3.

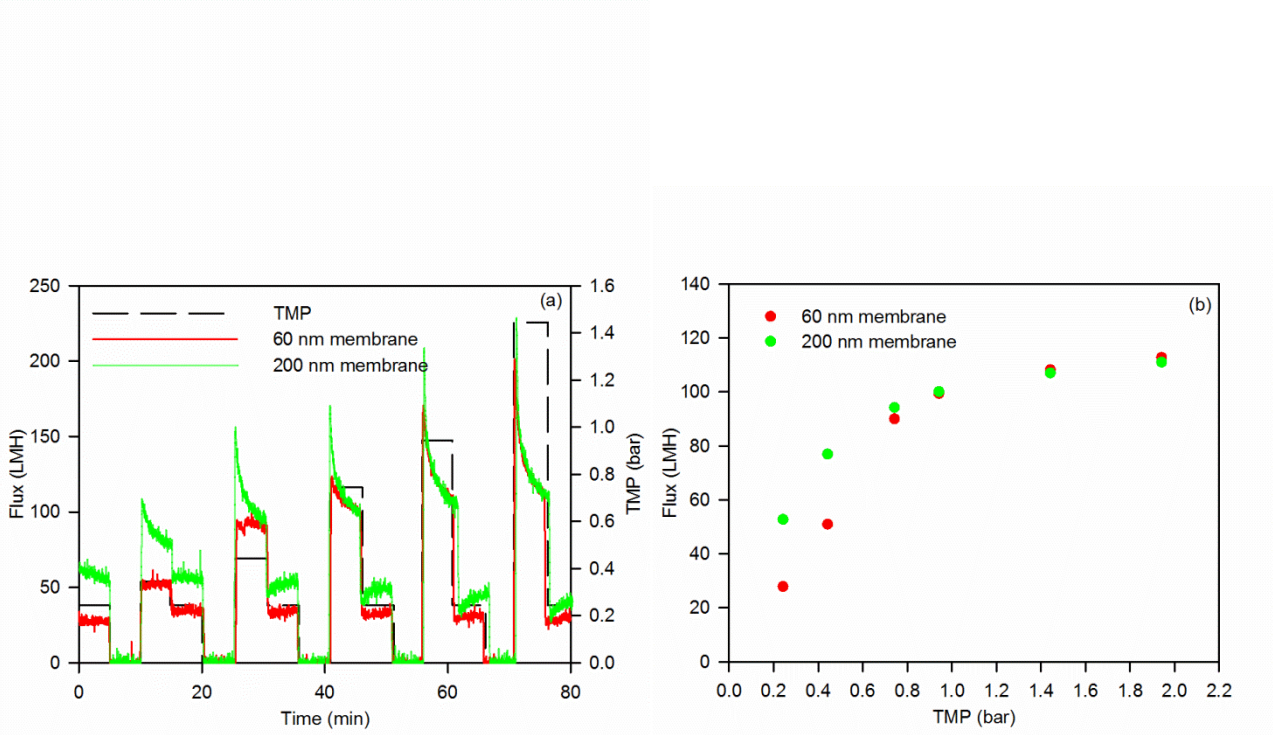

Figure 5.3: Flux measured on (a) flux and TMP over time in TMP step filtrations of sludge on membranes with average pore sizes of 60 and 200 nm, respectively, and (b) fluxes measured after 5 minutes of filtrations vs. TMP. Unpublished results.

The TMP-stepping approach used in Figure 5.3 uses gradually increasing pressure from 0.3 to 2 bar with 0.3 bar reference phases and 0 bar relaxation phases to restore permeability between each step. It is found that at the lower pressures (0.3 - 0.5 bar) of the TMP-step filtrations the fluxes measured on the 200 nm membranes are higher than the fluxes measured with the 60 nm membrane, which is due to the lower membrane resistance ($R_{m,\ 200\ nm} = 1.15 \cdot 10^{12}\ m^{-1}$, $R_{m,\ 200\ nm} = 1.15 \cdot 10^{12}\ m^{-1}$). The fluxes are higher at the 200 nm membrane in the pressure range 0.3-0.5 bar, but the fluxes declines over time in contrast to the steady fluxes measured with the 60 nm membrane. At the higher levels of pressure (0.8 - 2 bar), the 60 nm membrane also generates higher fluxes that declines over time, just as the 200 nm membranes. At these levels, the fluxes are found to decline towards the same values. This is observed when plotting the flux measured after 5 min against the pressure; the flux through the 60 nm membrane and the 200 nm membrane are the same. This shows that the development in flux at constant pressure is controlled by the mass balance in Eq. 5.2, hence the amount of cake and not the membrane permeability. As J_{LIM} is independent of pore size, the same back transport determines the decline in flux in the two systems, why the flux declines towards the same value, independent of pressure and membrane resistance. Increasing pressure will give a higher flux according to the Darcy equation, but will also generate more cake buildup and therefore give a faster decline in flux.

The flux in Figure 5.3 declines over time as $J > J_{LIM}$. Correspondingly, as the pressure is released the flux drops so $J < J_{LIM}$ which leads to flux restoration through the 200 nm membrane. At the 60 nm membrane, the flux remains constant at the 0.3 bar reference step, although $J < J_{LIM}$, because the membrane resistance is too high to give $J = J_{LIM}$ at 0.3 bar.

Therefore, the effect on flux by increasing pressure or having lower membrane resistance is limited as it is the formation of the cake and the back transport, J_{LIM}, which determines the level of flux.

5.2 Formation and removal of cake

In Paper I, II, IV and V it is shown that the limiting flux can be used to simulate the formation of cakes at different pressures with a modeling approach using Eq. 5.2. According to the mass balance, Eq. 5.2, the kinetics for formation and removal of cake depends on the limiting flux. As the limiting flux represents the effective average back transport from the membrane by the sludge components, it depends on operational parameters such as shear, and therefore membrane rotation speed, Ω. Therefore, the mass balance can model the development in flux at different operational conditions, by letting J_{LIM} represent the influence of different operational parameters e.g. shear.

In Paper II the development of cake is studied at different membrane rotation speeds on the sidestream filtation module filtrating lab scale MBR sludge. It is found that at higher rotation speeds the flux decline is lower and the levels of flux are generally higher. This is due to a linearly increasing limiting flux with rotation speed with rotation speed due to enhanced shear induced diffusion, giving a higher back transport and therefore less buildup described from Eq. 5.2 and illustrated in Figure 5.4. A linearly increment in J_{LIM} with rotation speed is also found in Paper I, and V.

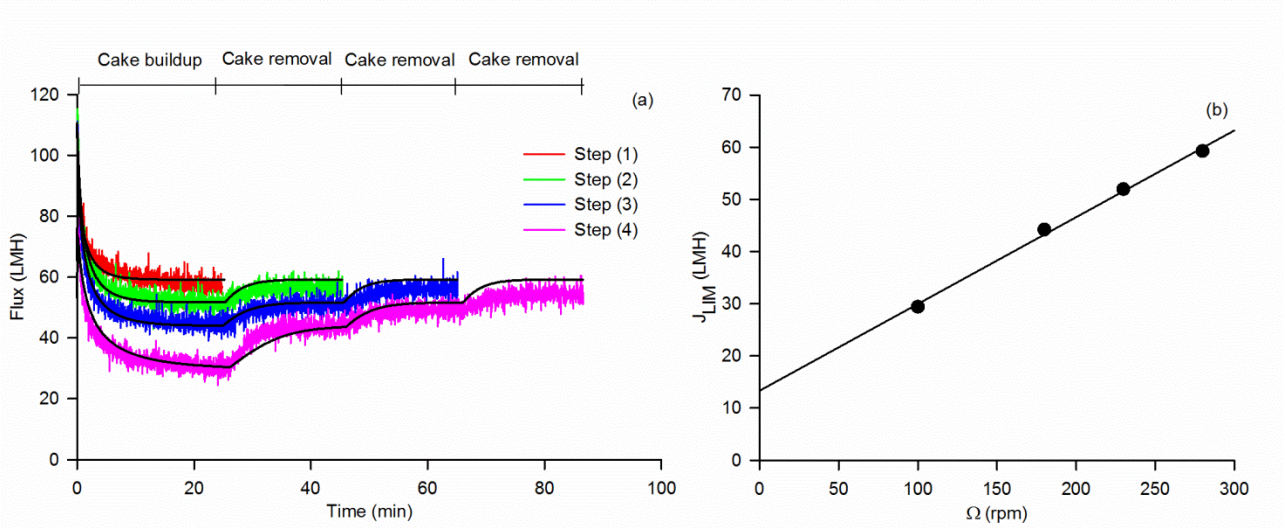

Figure 5.4: Flux over time in experiments with rotation stepping to reclaim flux (a) and limiting flux as function of rotation speed (b).

Not only does the formation of cake layers in short term experiments depend on J_{LIM} and the mass balance in Eq. 5.2, so does the removal of cake. This is shown in rotation stepping filtrations in Paper II, where cakes are formed at lower rotation speeds, and afterwards removed gradually by enhancing rotation speed. This was studied with four rotation stepping experiments, developed from Defrance and Jaffrin (1999b). The step experiments were performed at 1 bar TMP with the following conditions:

Step experiment 1. Cake buildup phase, 280 rpm for 25 min

Step experiment 2. Cake buildup phase, 230 rpm for 25 min → cake removal phase, 280 rpm for 20 min

Step experiment 3. Cake buildup phase, 180 rpm for 25 min → cake removal phase, 230 rpm for 20 min → cake removal phase, 280 rpm for 20 min

Step experiment 4. Cake buildup phase, 100 rpm for 25 min → cake removal phase, 180 rpm for 20 min → cake removal phase, 230 rpm for 20 min → cake removal phase, 280 rpm for 20 min

The recovered fluxes obtained when increasing rotation speeds corresponds to the limiting fluxes at the respective rotation speeds, found from cake development phases of the rotation stepping experiments. Furthermore, with the mass balance in Eq. 5.2, the development in flux in cake formation and cake removal phases is simulated well.

From this it is concluded that the mass balance can describe both the cake formation but also the cake removal on a membrane in a high shear MBR. Furthermore, as the cake formation and removal is described by this mass

balance, cake formation must be reversible. This is supported by the ability of enhancing shear to restore flux to the level of the limiting flux at the given rotation speed.

The removal of cake is also observed at the reference pressures of 0.3 bar in the filtration with the 200 nm membrane shown in Figure 5.3a. After fouling the membrane at a high pressure and lowering pressure to 0.3 bar, the lower driving forces gives a flux $J < J_{LIM}$, hence cake is removed. This is observed from the reclamation of flux in the 0.3 bar reference steps of the TMP stepping experiments. Similar results are observed in TMP step experiments in Paper I, IV and V.

5.3 Study of shear influence on J_{LIM} on a rotating membrane disc

The back transport described by the limiting flux is the sum of mechanisms of the variety of sludge components such as Brownian diffusion, shear induced diffusion, lateral migration and shear erosion of the cake [Belfort et al., 1994; Huismann and Trägårdh, 1999]. All these mechanisms depend of shear, giving a higher back transport at enhanced shear.

Several studies have developed models linking the enhanced shear or particle size or lower feed suspension concentration to higher back transport. These models are developed for membrane filtration of non-complex suspensions with a well-defined particle size of the foulants and geometry of the filtration module. Therefore, they will not be applicable for MBR systems, as the sludge is a complex mixture of different particles, colloids and macromolecules being affected by shear. Furthermore, the models, based on one or two dimensional particle transport governed by diffusion and convection in the crossflow direction, are inadequate to describe the complexity of flows near e.g. a hollow fiber or a rotating disc membrane module. Last but not least, the models linking shear to limiting flux have not described the effect of shear in non-Newtonian suspensions like MBR sludge.

Due to the complexity of activated sludge response to shear, empirical models have been developed to describe the effect of shear and concentration on limiting flux in MBR. Shimizu et al. (1996) has proposed the following model based on MBR filtration experiments with submerged hollow fiber modules:

$$J_{LIM} = A \cdot u^{*1.0} \cdot \varphi \cdot TSS^{-½} \qquad (5.4)$$

A is a filtration constant that represents the sludge filtration characteristics, u^* is the superficial air velocity, representing the effect of shear on the back transport of foulants, while φ is the geometric hindrance factor, a constant accounting for the complexity of a given filtration module.

In Paper III, a similar model is proposed, which will be presented in section *5.3.2. Model for limiting flux as function of rotation speed and radial distance*, and is based on experiments on rotating membrane discs. This study determines the shear stress from the shear rate with an expression valid for non-Newtonian fluids, and calculates the shear rate locally on the membrane to describe the radial effect of limiting flux and compare to experimental results. In the following, the shear on a rotating membrane disc will be described and linked to J_{LIM} obtained from experiments in Paper III.

5.3.1 Sludge rheology

The local shear rate in the area between an inner radius, r_i, and outer radius, r_o, on a rotating membrane disc, can be described as function of rotation speed from the following expression [Bouzerar et al., 2000; Jaffrin, 2008].

$$\dot{\gamma}_m = 0.5133 v^{-0.5} (k\Omega)^{1.5} \frac{r_o^3 - r_i^3}{r_o^2 - r_i^2} \tag{5.5}$$

v is the kinematic viscosity of the feed suspension and k is a velocity factor with $k = 0.42$ for flat discs. The expression is valid for laminar flow regimes. In Paper II it is shown that the flow regime is laminar for rotation speeds 100-280 rpm at 11 g/L sludge. The sludge viscosity depends on sludge concentration and shear rate, due to its non-Newtonian behavior. The apparent dynamic viscosity, μ_a (mPa·s), of MBR sludge can be determined from the following expression [Rosenberger et al., 2002].

$$\mu_a = exp(2TSS^{0.41}) \dot{\gamma}^{-0.23TSS^{0.37}} \tag{5.6}$$

With higher TSS the sludge viscosity increases, while increasing shear rate leads to lower viscosity due to shear thinning. The kinematic viscosity, v, is calculated from the following equation:

$$v = \frac{\mu_a}{1000 \rho_s} \tag{5.7}$$

ρ_s is the sludge density and it is assumed that ρ_s = 1040 kg·m^{-3}. Inserting the kinematic viscosity of sludge into Eq. 5.5 has the solution for the membrane shear rate:

$$\dot{\gamma}_m = \left(0.5133 \left(\frac{1}{1000 \rho_s} exp(2TSS^{0.41}) \right)^{-0.5} (k\Omega)^{1.5} \frac{r_o^3 - r_i^3}{r_o^2 - r_i^2} \right)^{1/1 - 0.115TSS^{0.37}} \tag{5.8}$$

From the shear rate, the shear stress, τ, of a non-Newtonian fluid is described through the following non-linear relationship [Rosenberger et al., 2002; Laera et al., 2007; Pollice et al., 2007].

$$\tau = m\dot{\gamma}^n \quad (5.9)$$

m is the fluid consistency index and *n* is the flow behavior index ($n < 1$). Both parameters are functions of TSS:

$$m = 0.001exp(2TSS^{0.41}), n = 1 - 0.23TSS^{0.37} \quad (5.10)$$

Therefore, from Eq. 5.8 and 5.9 the shear stress on rotating membrane discs is calculated in Paper III as function of radial distance, rotation speed and sludge concentration, presented in Figure 5.5.

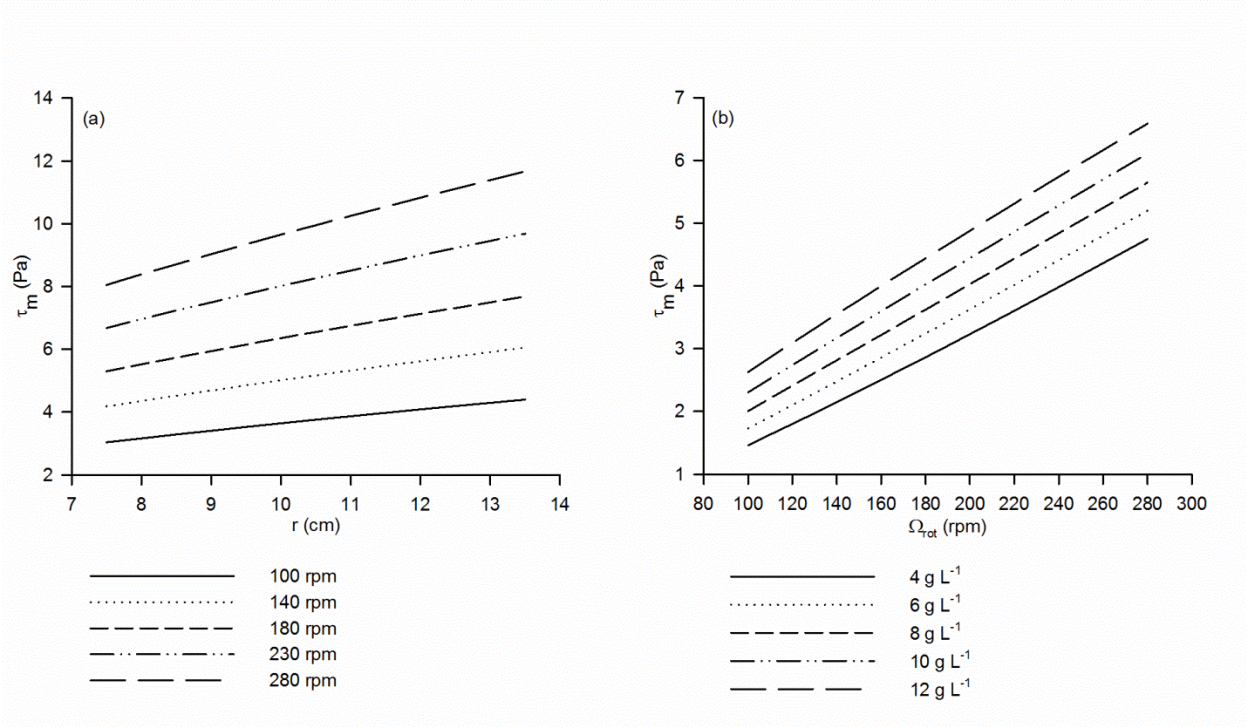

Figure 5.5: Shear stress as function of radial distance from center of rotation at different rotations speeds (a) and shear stress vs. rotation speed at varying sludge concentrations (b).

It is found that the shear stress increases with radial distance as expected, because the azimuthal velocity increases with both parameters. The shear stress increases with higher sludge concentrations as a more viscous liquid is stressed more by the same mechanical movement. The tendency and level of the shear stress are in accordance with a study by Ratkovich et al. (2012b), who from CFD simulations found increasing shear stress with increasing sludge concentration and rotation speed of rotating impellers near a membrane.

The shear stress created from air scouring in MBRs generally lower, with average shear stresses on the membrane in the range of 0.25 – 0.5 Pa and also value as high as 2 Pa [Van Kaam et al., 2006; Ratkovich et al.,

2012a]. This is a consequence of the air scouring only affecting parts of the membrane at once, i.e. where the bubbles are, and that the liquid movement relative to the membrane enhanced by rotation is higher.

5.3.2 Model for limiting flux as function of rotation speed and radial distance

With background in the shear stress, a model for limiting flux as function of shear and concentration is proposed in Paper III. The model assumes the same linear relationship between limiting flux and TSS. Accepting that the shear dependent mechanisms giving back transport of foulants is a combination of shear induced diffusion, Brownian diffusion, erosion, and parameters like boundary layer thickness etc., a non-linear relationship between limiting flux and shear stress is proposed. This has also been done in other studies, where the shear stress has an exponent *B* that represents the effect of the module geometry on the back transport [Ghogomu et al., 2001; Moll et al., 2007]. Therefore, the proposed model has the following form.

$$J_{LIM} = A \cdot {\tau_m}^B TSS^{-½} \qquad (5.11)$$

A is a sludge specific constant, comparable to the constant proposed by Shimizu et al. (1996), that describes the sludge mixtures response to shear depending on the sludge characteristics, e.g. particle size, particle size distribution.

The model was fitted to experimental data of limiting fluxes obtained at different rotation speeds and at different concentric rings of the membranes. The model showed to be able to simulate the increasing J_{LIM} with higher shear obtained from increasing rotation speed and radial distance.

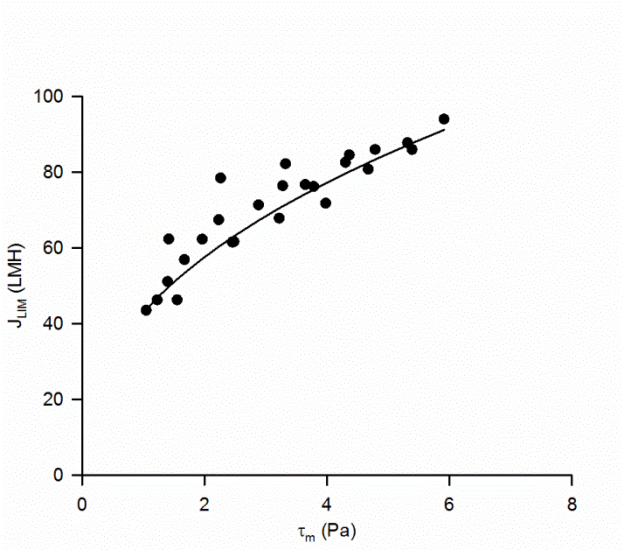

Figure 5.6: Experimental (●) and modeled (-) limiting flux as function of shear stress on a membrane disc at varying rotation speeds in different concentric discs of the membrane.

The solution for the RMSE fitting procedure of modeled to experimental J_{LIM} gave $A = 3.77 \cdot 10^{-5}\ kg^{0.5} \cdot m^{-0.5} \cdot s^{-1}$ and $B = 0.42$. As B < 1 there is an un-linear increase in limiting flux with shear stress, with a decreasing slope with higher shear stress. This has also been observed in other studies of shear influence on back transport in micro and ultrafiltration of suspensions [Ghogomu et al., 2001; Moll et al., 2007].

5.4 Influence of concentration on J_{LIM}

From the mass balance in Eq. 5.2 it is deducted that the back transport depends on the concentration gradient between the bulk and membrane/cake wall. As the stagnant cake has formed on the membrane surface, concentration gradient varies only with bulk concentration. Therefore, increasing bulk concentration gives a lower back transport of foulants. This has been confirmed in various studies, where higher concentrations has shown to give lower back transport or lower levels of flux due to higher fouling [Davis and Sherwood, 1990; Shimizu et al., 1996; Meng et al., 2007].

In Paper III the development in J_{LIM} vs. membrane rotation speed was studied for different sludge concentrations, shown in Figure 5.7.

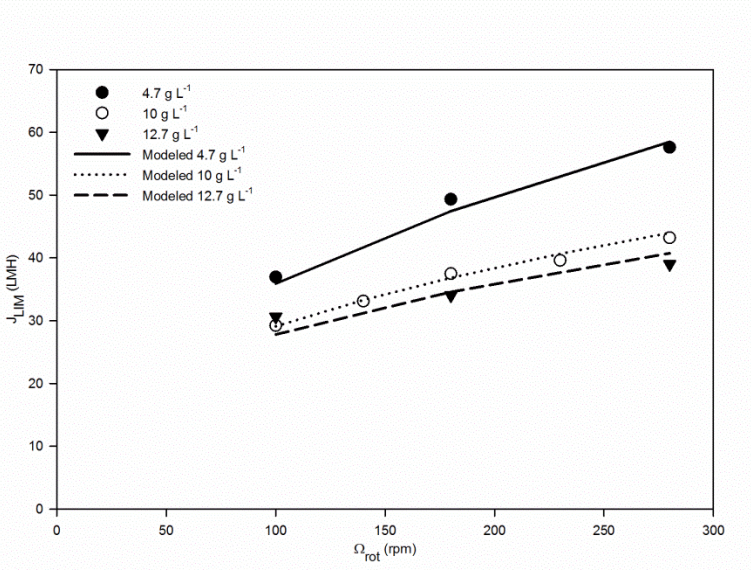

Figure 5.7: Measured and modeled flux as function of rotation speed at different sludge concentrations.

Sludge (10 g/L) was either diluted with permeate or concentrated by settling, to keep sludge characteristics, such as conductivity and particle size distribution, constant during filtration of three different sludge concentrations. Modeling TMP step experiments gave limiting fluxes vs. rotation speed for the series of different sludge concentrations, showing lower limiting flux with higher TSS, which is in accordance with theory and observations in literature. The limiting fluxes obtained at different rotation speeds and sludge concentrations were fitted to the proposed model for limiting flux, Eq. 5.11. This showed that the model was actually able to simulate the lower levels of limiting flux found experimentally with higher sludge concentration. The sludge filterability in terms of CST was lower in the series of experiments presented in Figure 5.7 than the experiments presented in Figure 5.6. This is reflected in a lower filtration constant *A*, while the same exponent *B = 0.42* was able to represent the influence of shear on the back transport in both types of sludge. Hence, the exponent *B* seems to be a sludge independent parameter, describing the influence of either module geometry or combined effect of different back transport mechanisms.

Therefore, with Eq. 5.11 the limiting flux can be determined as function of membrane rotation speeds and concentration in the range 100 - 280 rpm and 4.7-12.7 g/L. As it only is the filtration constant, *A*, that depends on sludge characteristics the limiting flux can be normalized with the limiting flux found from 12.5 g/L sludge at 100 rpm membrane rotation speed, to find the significance of enhanced rotation speed and variations in sludge concentration on the back transport.

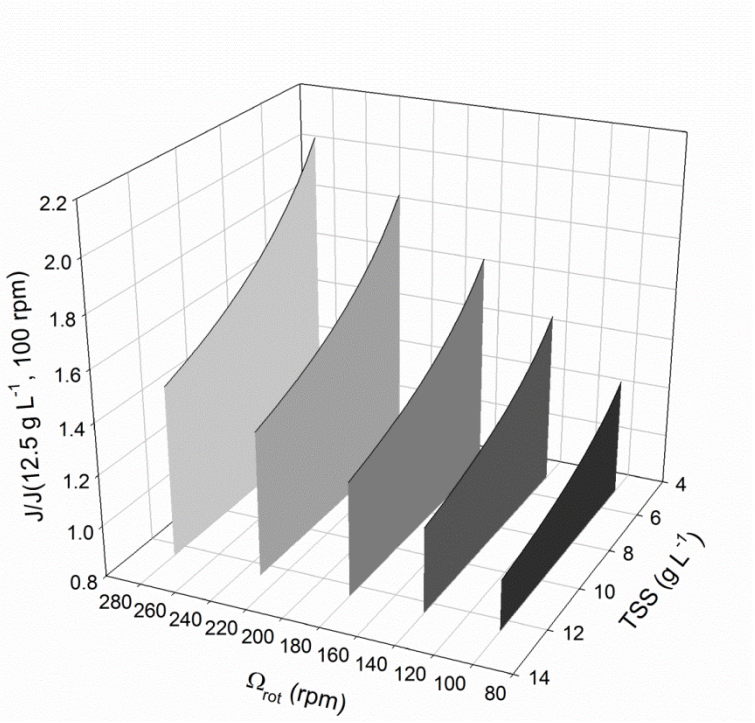

Figure 5.8: Normalized limiting flux with J_{LIM}(12.5 g/L, 100 rpm) as function of rotation speed and sludge concentration. From Paper III.

In Figure 5.8 it is shown, that going from 100 to 280 rpm at 12.5 g/L the flux increases with around 60 %, while going from 12.5 g/L to 5 g/L TSS gives a 20% increase in J_{LIM}. However, this does not mean that the permeate production is only 60% higher by increasing the rotation speed with a factor 2.8. Consider a system, where the initial permeate flux is 100 LMH at a given pressure and J_{LIM} is 50 LMH. Hence, $d\omega_c/dt = (100\text{-}50)\cdot TSS = 50\cdot TSS$. Increasing the back transport with 60 % gives J_{LIM} = 80 LMH, hence $d\omega_c/dt = (100\text{-}80)\cdot TS = 20\cdot TSS$. Hence, there will be a significant influence on the fouling rate and permeate production, as the decline in flux over time is slower. Therefore, more permeate will accumulate at the higher shear levels.

Bugge et al. (2011) has observed a more complex link between flux and TSS in TMP stepping experiments with a submerged membrane module with air scouring for shear. Here it was observed that the lowest of three sludge concentrations had the lowest flux. Also, Loussada-Ferreira et al. (2010) observed with DFCm filtrations, that there was an optimal concentration of 10 g/L MLSS for filterability, with lower filterability at higher concentrations and lower filterability at lower concentrations. This suggests that the back transport in MBR systems can be more complex than just a shear induced diffusion phenomenon. Instead it could also be an effect of increased erosion of the fouling layer by the higher number of foulants streaming along the membrane surface giving higher fluxes.

6. Cake compression

6.1 Pressure dependency of specific cake resistance

For cake filtration, it is well established that the specific resistance of a filter cake is pressure dependent. This is explained by the compressibility of filter cakes, where increasing pressure gives a higher specific cake resistance, because of deformation of e.g. soft sludge flocs and rearrangements in the cake structure [Christensen, 2006]. Conversely, lowering pressure gives a lower specific cake resistance, i.e. the cake swells back with some degree of reversibility.

The specific cake resistance pressure dependency has been described by Tiller and Yeh (1987) with the following empirical equation:

$$\alpha = \alpha_0 \left(1 + \frac{\Delta P_c}{P_a}\right)^{\beta} \qquad (6.1)$$

α_0 is the specific cake resistance at no pressure, ΔP_c is the pressure drop over the cake, P_a is a compressibility parameter, and β is an empirical constant that equals 1 for highly compressible structures such as sludge cakes [Sørensen and Sørensen, 1997b; Tiller and Kwon, 1998]. Hence, for sludge cakes there is a linear increment in specific cake resistance with pressure. In this case, P_a denotes the pressure required to obtain $\alpha = 2 \cdot \alpha_0$, thus a lower P_a value represents a higher compressibility.

An alternative relationship between specific cake resistance and pressure is given in [Tiller et al., 1972]

$$\alpha = \alpha_0 \cdot \Delta P_c^{\beta} \qquad (6.2)$$

In contrast to Eq. 6.1, Eq. 6.2 does not describe the specific cake resistances present at $\Delta P_c = 0$.

It has been shown that sludge filter cakes are subject to creep deformation [Christensen and Keiding, 2007]. Therefore, when applying a pressure to a filter cake the specific cake resistance changes gradually towards the specific cake resistance that applies to the given pressure, defined by Eq. 6.1. This time dependent change in specific cake resistance can be modeled numerically from the following first order equation.

$$\alpha_t = \alpha_{t-1} \Delta t \left(\alpha_{eq.} - \alpha_{t-1}\right) k_a \qquad (6.3)$$

α_t is the specific cake resistance at time t, α_{t-1} is the specific cake resistance at the previous time step, Δt is the length of the time step and k_a is a constant describing the kinetics of compression.

It has been shown, that the principles of cake compressibility developed for dead-end cake filtration can be applied for describing fouling layers in membrane filtration as well [Sørensen and Sørensen, 1997a; Christensen et al. 2009]. For self-forming dynamic membrane bioreactors, compressibility of the sludge cakes has also been observed [Liang et al., 2012]. In one study, it was found that the development in fouling in membrane bioreactors could be simulated from cake buildup and cake compression with a relationship between α and ΔP_c described from Eq. 6.2 [Giraldo and LeChevallier, 2006]. However, no direct observation of compressibility of sludge fouling layers on the membrane was observed in terms of changes in cake resistance with pressure.

6.2 Observations of cake compressibility

The compressibility is studied through the cake resistances pressure dependency. As an example, the result from a filtration of 10 g/L MBR sludge from a pilot MBR at Aalborg Vest WWTP with a 0.2 µm average pore size PVDF flat sheet membrane is presented. TMP was changed to vary between 8000 and 13700 Pa in 5 minutes intervals. From the measured permeate fluxes, the cake resistance was calculated with the Darcy equation, Eq. 2.1, and plotted over time in Figure 6.1.

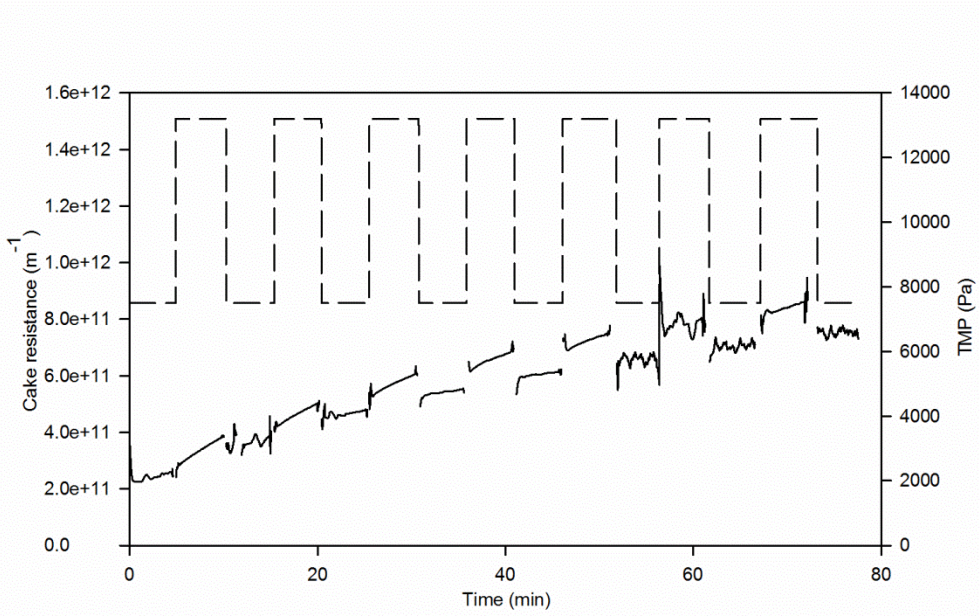

Figure 6.1: Cake resistance (solid line) and TMP (dashed line) during filtration of sludge with a HS polymeric membrane and TMP varying in 5 min intervals. Unpublished results.

The figure shows that the cake resistance increases gradually over time due to cake formation. As pressure increases, the cake resistance jumps to a higher level. The cake resistance drops as pressure is lowered to 8000 Pa. At higher level of cake resistance, the more significant is the change in cake resistance when changing

pressure. However, the percent-wise increase in cake resistance does not change with the level of cake resistance before pressure change, but remains constant. This is in agreement with Eq. 6.1, as a change in pressure shall give a consistent change in specific cake resistance and thereby cake resistance.

In Paper I and Paper V it is shown through experiments on a rotating membrane disc filtrating lab scale MBR sludge, that the change in pressure has different impact on the cake resistance through the cake buildup and cake compression in TMP step experiments. This is explained from Figure 6.2.

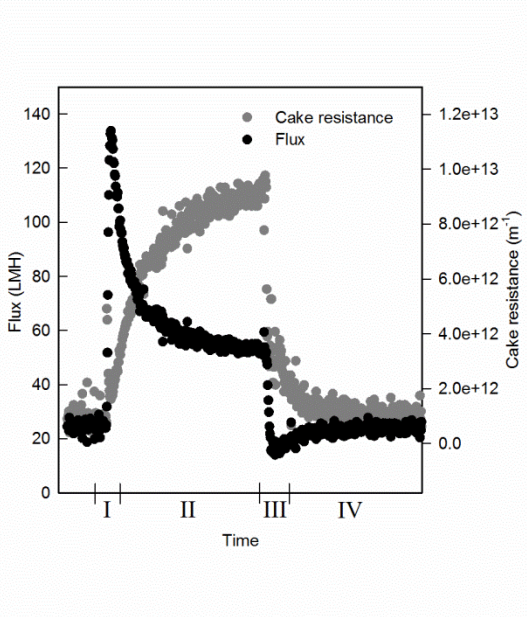

Figure 6.2: Development in flux and cake resistance over time as TMP is stepped up and down. The development is divided into four phases; Phase I showing the initial compression of sludge cake and buildup, Phase II representing the cake buildup where the flux decreases towards a steady state, Phase III where TMP is lowered and cake resistance declines rapidly, and Phase IV where the flux increases as $J < J_{LIM}$.

The figure shows the development in flux and cake resistance at a high (compressive) and a low pressure. The development is divided into four phases; Phase I and II occurring during the high pressure and phase III and IV at the low pressure. The four phases are elaborated in the following:

I. When increasing pressure, the flux has a high offset due to enhanced driving forces, but declines dramatically due to the increase in cake resistance (dR_c/dt) from cake buildup ($d\omega_c/dt$) and compression ($d\alpha/dt$).

II. Flux declines toward a steady state due to cake buildup. The cake is not compressed further at the constant pressure.

III. Flux declines drops as the driving force is lowered. Cake resistance also drops, partly due to swelling of the cake as TMP is released and partly due to cake removal.

IV. The lower TMP gives a flux lower than J_{LIM}, which, if cake buildup is reversible, leads to cake removal and thereby restoration of permeability.

6.3 Reversibility of cake compression

When pressure on a compressed cake is released the cake swells back if the cake compression is reversible. The reversibility of compression of a cake layer on rotating membrane discs filtrating sludge from the pilot scale MBR system have been investigated in Paper II. As pressure is released on the compressed fouling layer, two mechanisms can give lower cake resistance: First, as the flux drops, $J < J_{LIM}$ which leads to cake removal according to Eq. 5.2. Second as the pressure is reduced, Eq. 6.1 predicts a lower specific cake resistance, hence cake swelling. Hence, the decline in cake resistance can be an effect of cake removal, cake swelling or a combination of both mechanisms. It is difficult to separate the effect from cake buildup and compression from *J - TMP* data alone, as both factors affects R_c through Eq. 2.3.

To study out whether the drop in cake resistance is due to cake removal or swelling, a set of experiments were designed in Paper II to only see the compressibility effects on the cake resistance when lowering pressure. This has been done by performing two set of experiments. In one set, the development in flux when changing the pressure from 0.8 bar up to either 1.2, 1.4 or 1.6 bar and back to 0.8 bar again at a constant rotation speed of membrane discs. At the second set of experiments, the goal was to isolate the effects of pressure on the cake layer structure on the cake resistance. This was done in an attempt to keep cake buildup constant. The same procedure for changes in flux was used, but when lowering pressure to 0.8 bar, the mass balance determining cake buildup (Eq. 5.2) was manipulated by lowering the back transport, hence J_{LIM}, with the same degree, as the flux was known to drop, determined from the first set of experiments. The appropriate J_{LIM} was obtained by lowering membrane rotation speed.

The result of this study is that the reduction of flux is in the same range for the set of experiments with constant back transport as in the experiments with varying back transport, hence constant cake buildup when lowering pressure. The development in cake resistance in the two set of experiments at 1.2 bar compressive pressure is shown in Figure 6.3.

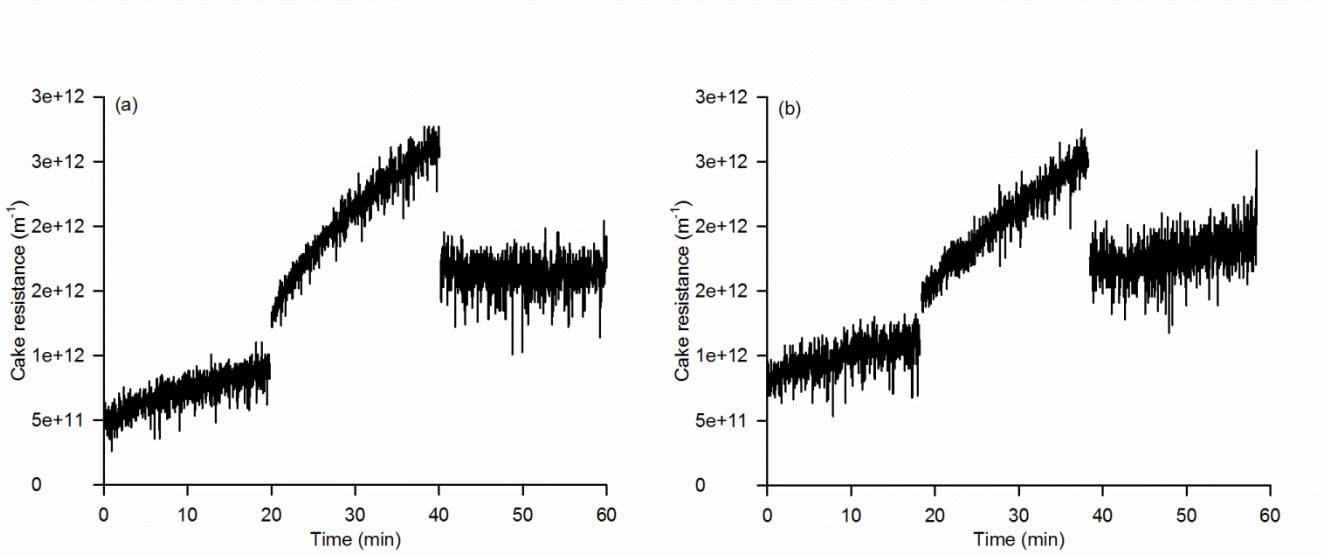

Figure 6.3: Development in cake resistance in a TMP step experiment with constant rotation speed (a) and lowered rotation speed in the swelling phase to keep cake buildup constant when lowering pressure.

Both set of experiments show increasing cake resistance with time as the sludge cake is forming. Increasing pressure gives a jump in cake resistance and a faster increment in cake resistance due to cake compression and buildup, respectively. As pressure is released, the cake resistance drops in the experiments with constant back transport and in the experiments with reduced back transport to keep cake buildup constant. The drop in cake resistance is of the same magnitude; the only difference is that the cake resistance in the last set of experiments increases over time, as $J > J_{LIM}$. Therefore, it is concluded that the instant drop in cake resistance is a result of cake swelling rather than cake removal.

From this it can be concluded, that the cake compression predominantly is reversible and that the kinetics of cake compression and swelling are faster than the kinetics of cake buildup and removal.

This study shows that characterizing cake compressibility is complicated by the dual effects of change in amount of cake and change in cake structure that influences cake resistance as pressure is changed. In Paper VI, the real-time characterization of cake compression was extended by use of monitoring sludge on-line with and ultrasonic sensor, which did show signs of changes in cake structure, as pressure was changed. This will be explained further in Chapter 8.

6.4 Operational parameters influence on compressibility

In Paper I, II and V, the pressure dependency of the cake resistance is found in TMP step experiments. In Paper V, the compressibility of cakes formed on rotating membrane discs filtrating lab scale MBR sludge, was found for varying rotation speeds with a modeling approach described in the next chapter.

Table 6.1: Cake compressibility parameters obtained from filtrations at different membrane rotation speeds. Data obtained from Paper V.

Ω_{rot} (rpm)	α_0 (m/kg)	P_a (Pa)	k_α
100	$2.52 \cdot 10^{13}$	19700	0.031
140	$2.63 \cdot 10^{13}$	22700	0.033
160	$2.63 \cdot 10^{13}$	26450	0.033
180	$2.48 \cdot 10^{13}$	28701	0.034
205	$2.75 \cdot 10^{13}$	32300	0.040
230	$2.95 \cdot 10^{13}$	32500	0.047
280	$3.00 \cdot 10^{13}$	35100	0.089

It is observed from Table 6.1, that there is a tendency for increasing α_0 with increasing rotation speed/shear, i.e. an initially more compact layer. Furthermore, P_a values for cakes formed at high shear are higher than those formed at lower shear. Hence, the cakes become less compressible but have a higher specific cake resistance at higher rotation speeds. This is explained with the principle of selection of the depositing sludge components, illustrated in Figure 6.4.

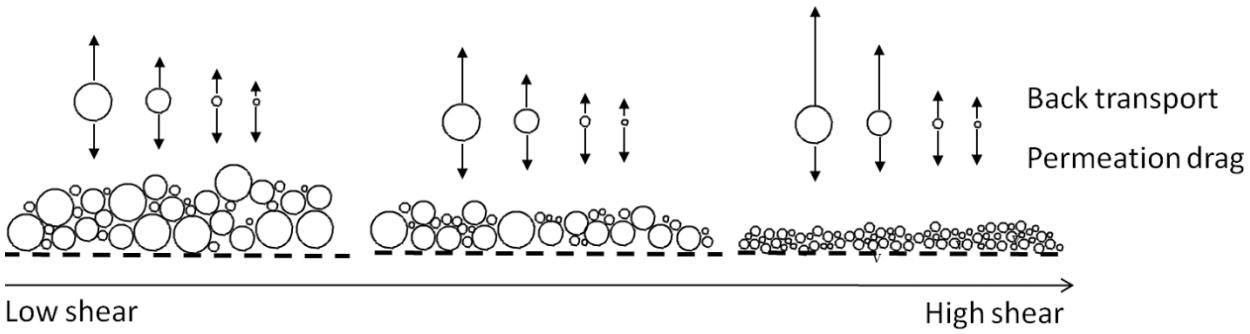

Figure 6.4: Illustration of the effect of enhanced shear and particle back transport on the selection of particles depositing on the membrane and cake structure.

Particles and large colloids are more affected by shear induced diffusion, supported by Figure 2.2. Therefore, at higher levels of shear there will be a selection of smaller colloids and particles depositing on the membrane and thus a different structure of the cake layer [Davis and Sherwood, 1990; Ripperger and Altmann, 2002].

Smaller particles form denser layers with lower porosity that have lower permeability (higher α_0) but are less compressible (higher P_a) than cakes consisting of larger particles [Lee et al., 2006; Li et al., 2012a]. Therefore, the selection of smaller particles at higher shear levels can explain the increase in α_0 and P_a that follows enhanced rotation speed.

The selection of particles at varying shear levels can potentially be used to engineer the fouling layer characteristics. In a study by Pollet et al. (2009) it was shown that discontinuous aeration (i.e. shear) enhanced the filtration properties of fouling layers formed in MBR. During the periods with a low air scouring, hence low shear, a fouling layer with lower density was formed. This could easily be removed during the high aeration periods due to the low fouling layer density. The formation of loose-structured cake layers has been shown to an effective fouling control strategy, as a loose structure cake layer has a low porosity, hence low α_0, is reversible and protects the membrane surface from soluble substances forming irreversible fouling [Wu et al., 2012].

7. Modeling and monitoring cake buildup and compression

7.1 Model structure

The effects of cake buildup and cake compression on membrane resistance described in the previous chapter have been combined into one model to simulate the development in fouling in MBR. The developed approach was presented in Paper I and IV and used to simulate data from TMP step experiments from a sidestream MBR system with rotating membrane discs (Paper I, II and IV) and a system with flat membranes submerged in MBR sludge (Paper V). The modeling approach is outlined in Figure 7.1. The modeling is divided into seven steps, which are explained under the figure.

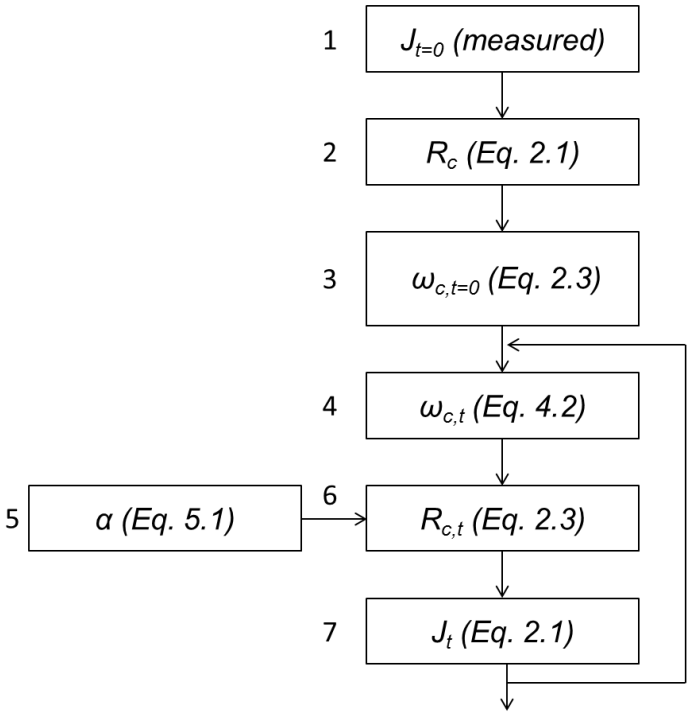

Figure 7.1: Dynamical Euler modeling approach to calculate the development in flux over time.

In case that the membrane resistance at the start of the filtration experiment is different from the clean membrane resistance, a start amount of cake will be estimated through step 1-3. This is done with emphasis on the first measured flux to calculate a start amount of cake from Eq. 2.1 and Eq. 2.3 using α for the specific pressure. In this procedure, it is assumed that the extra resistance is due to formation of a sludge cake. On the basis of this amount of cake, the development in amount of cake is calculated using Eq. 5.2 (step 4).

The time step for modeling is set to 1 sec, which corresponds to the rate of logging permeate flow in most experiments. As input flux for the mass balance in Eq. 5.2, the flux for the previous time, $J_{t-\Delta t}$, is used. In Paper I, frequent relaxation phases were applied to restore flux, which can be expected to give low amounts of fouling, i.e. $\omega < \omega_{crit}$. Therefore, the back transport cannot be expected to be constant at the relaxation phases. As $J_{BT} \neq J_{LIM}$, Eq. 5.3 replaces the J_{BT} term in Eq. 5.2 to describe the back transport as a function of fouling. With this methodology the model was able to simulate the regeneration of flux after relaxation phases. In Paper V on the other hand, it could be assumed that $J_{BT} = J_{LIM}$ as there are no relaxation phases to remove fouling and $\omega > \omega_{crit}$.

From the given pressure applied to the cake at time *t*, the specific cake resistance is calculated from Eq. 6.1 (step 5). For the polymeric flat sheet membranes used in the lab scale MBR in Paper IV, the pressure used to calculate α was $\Delta P_c = TMP$, as the resistance of the membrane was negligible compared to the resistance of the fouling layer. On the contrary, in studies using ceramic membrane discs for filtration, e.g. Paper I, the pressure drop over the cake was calculated from equation 7.1, as the resistance of the ceramic membrane discs was high enough to give a significant pressure drop, giving a lower effective pressure on the cake.

$$\Delta P_c = TMP - \mu R_m J_{t-\Delta t} \qquad (7.1)$$

In Eq. 7.1 the term, $\mu R_m J_{t-\Delta t}$, represents the pressure drop over the membrane.

In Paper IV and V it is shown, that the dynamics of cake compression in TMP step experiments without total relaxation gives a better fit, if Eq. 6.3 was used to describe the creep effect of cake compression. This was not necessary for the TMP step experiments designed for Paper I, as relaxation phases were applied to remove cake. As there were only low amounts of cake (if any) present after relaxation, this time dependent response was not required to describe the compression, unlike Paper IV and V, where the cake was still on the membrane before compressing it.

From the product of the amount of cake and the specific cake resistance, Eq. 2.3, the cake resistance at time *t* is determined (step 6) and from this the flux at time *t* is calculated with Eq. 2.1 (step 7). Step 4-7 are repeated to calculate the development in amount of cake, specific cake resistance and permeate flux numerically over time.

A fit of modeled flux to measured flux in a TMP step experiment with relaxation on rotating membrane discs in synthetic MBR sludge from Paper I is presented in Figure 7.2.

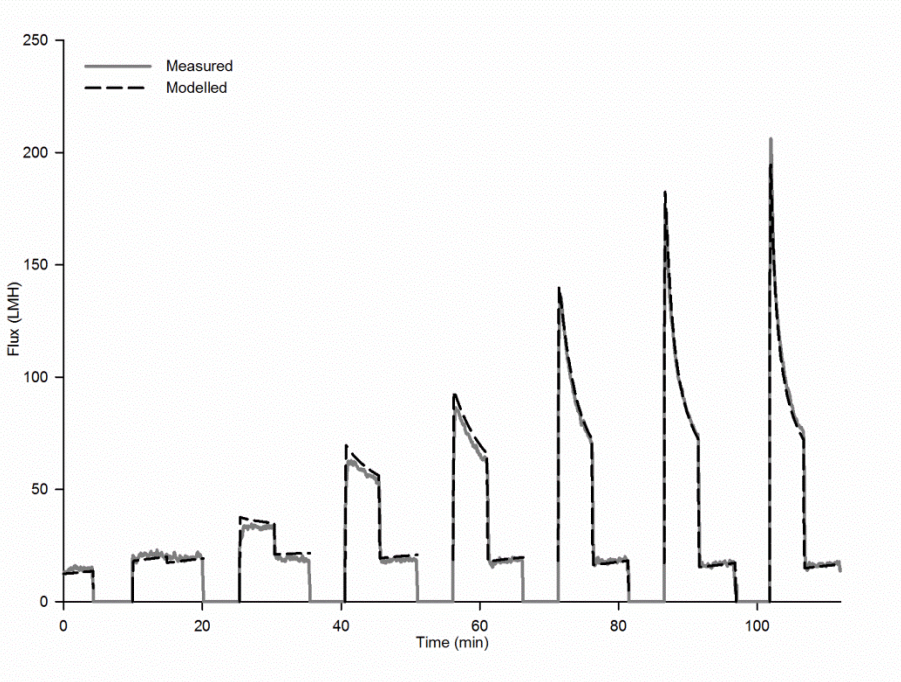

Figure 7.2: Development in measured (solid line) and modeled flux (dashed line) over time in a TMP step experiment. From Paper I.

The figure shows that the flux is well simulated during the cake buildup phases at high pressures and also during cake removal at low pressures ($J < J_{LIM}$). Furthermore, the flux restoration after relaxation is described well with the cake removal term as the initial flux after relaxation is simulated well. When comparing modeled fluxes to experimental fluxes it is assumed that the formation of fouling is homogenous over the membrane surface, hence that the averaged measured flux and TMP data can be can represent the development in fouling, described by the model.

The use of $\Delta t = 1\ sec$ as the step size is evaluated in Figure 7.3. Here, the accumulated volume of permeate relative to the membrane area after 1 h of filtration at 1 bar pressure is simulated with parameters from Paper I. This is done at different time steps giving a varying number of steps, with $\Delta t = 1\ sec$ corresponding to 3600 number of steps for 1 h of filtration.

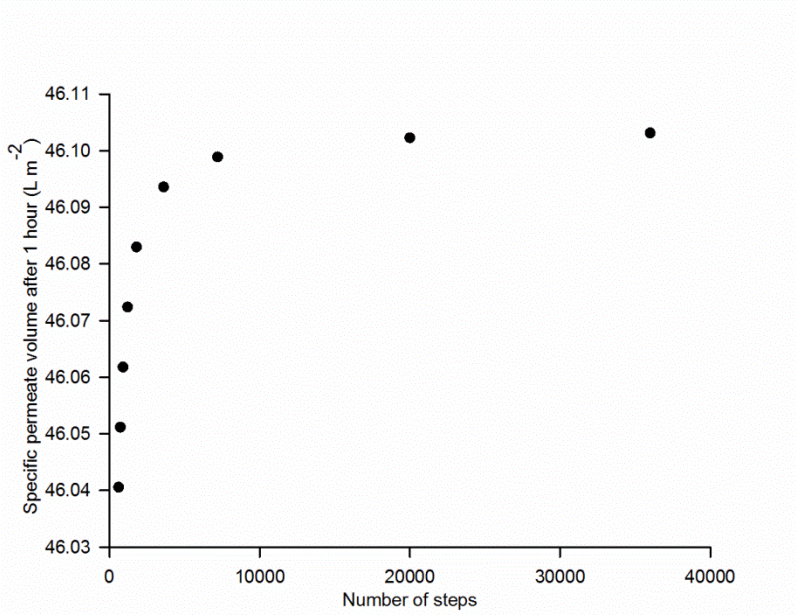

Figure 7.3: Produced volume of permeate relative to membrane area at varying number of steps for numerical modeling.

It is observed from the figure, that increasing the number of steps gives an increasing predicted specific permeate volume. This seems to level off at a number of steps higher than 3600. Thereby, to reduce numerical error, the time step should not be larger than $\Delta t = 1\ sec$. It is concluded from the figure, that the simulations of the model are relatively stable with the time steps used.

7.1.1 Fitting process

The input parameters for the model are the following constants:

- μ
- TSS
- R_M
- TMP

The basic fitting parameters of the model are:

- J_{LIM}
- α_0
- P_a

These parameters are constant and independent of pressure throughout the entire TMP step experiment. They are changed with the RMSE method to give the best fit of modeled flux to measured flux throughout the TMP step experiments. Before changing the fitting parameters, reasonable starting values are used as a guess for the actual value in order to obtain a fit with reliable parameter values.

A good approximation of J_{LIM} can be obtained from the decline in flux over time. However, giving a reasonable estimate of the compressibility parameters is less straightforward. In Paper I and IV an approach is developed to estimate α_0 and P_a from analysis of the development in cake resistance with changing pressures.

Once the best fit of the simulated to the experimental flux has been obtained by fitting the parameters J_{LIM}, α_0 and P_a, Eq. 5.3 and Eq. 6.3 are introduced, if necessary, and the parameters ω_{crit} and k_a fitted.

7.1.2. Estimation of α_0 and P_a

Approach A

Analysis of the change in cake resistance before and after changing pressure is used in Paper I, IV, and V to estimate the specific cake resistance pressure dependency, and from this give an estimate of α_0 and P_a.

The relative change in cake resistance from R'_c to $R_{c,ref}$ when changing the pressure drop over the cake from $\Delta P'_c$ to $\Delta P_{c,ref}$ is described with the following equation:

$$\frac{R'_c}{R_c} = \frac{\left(1+\frac{1}{P_a}\Delta P'_c\right)}{\left(1+\frac{1}{P_a}\Delta P_{c,ref}\right)} \cdot \frac{\omega'_c}{\omega_c} \tag{7.2}$$

If the change in pressure is instant, e.g. a few seconds, the change in amount of cake can be assumed to be negligible and the relationship between the amount of cake before and after compression can be assumed to be the same. With this assumption, Eq. 7.2 is reduced to:

$$\frac{R'_c}{R_c} = b + a\frac{\Delta P'_c}{\Delta P_{c,ref}} \tag{7.3}$$

Eq. 7.3 is a linear relationship with a slope, *A*, and intersection, *B*, from which P_a can be determined:

$$P_a = \Delta P'_{c,ref}\frac{b}{a} \tag{7.4}$$

where $b = \frac{1}{1+\frac{\Delta P_{c,ref}}{P_a}}$ and $a = b\frac{\Delta P_{c,ref}}{P_a}$.

The concept of this analysis is given in Figure 7.4

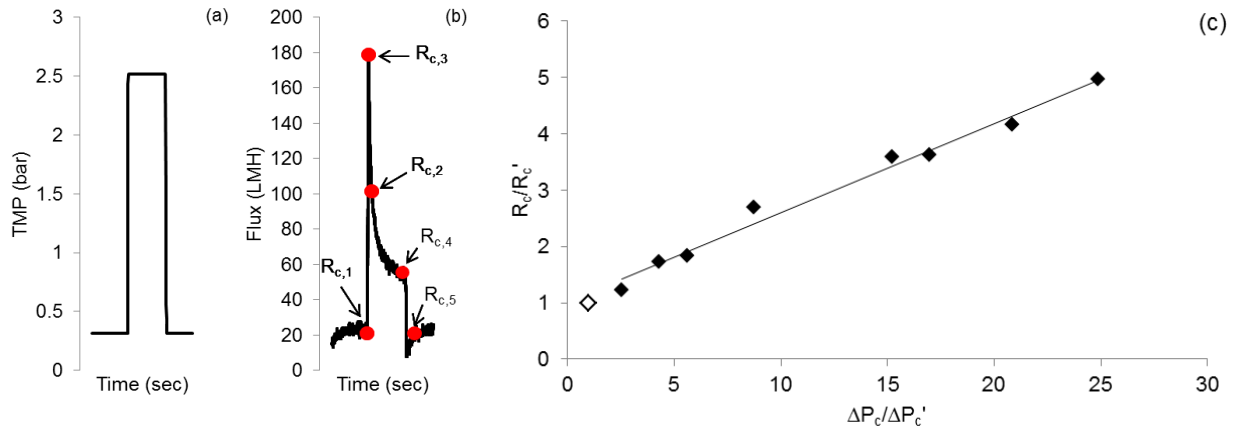

Figure 7.4: Change in TMP (a) and associated change in flux and cake resistance (b). From the change in cake resistance before and after changing pressure, P_a can be determined through a linear regression of the relationship of the change in cake resistance before and after change in pressure applied to the cake (c). The empty marker represents (1,1) where the line should intersect, as no change in pressure should give no change in resistance.

In Figure 7.4 it is shown, that from a TMP step experiment, the response of the cake to pressure changes can be studied either when compressing the cake or swelling the cake. In Paper I it is shown how P_a can be determined from the swelling, i.e. the change in resistance from $R_{c,4}$ to $R_{c,5}$, while in Paper IV and V it is possible to determine the change in cake resistance when compressing the cake by comparing the change from $R_{c,1}$ to $R_{c,2}$, illustrated in Figure 7.4. The resistance $R_{c,2}$ is used instead of $R_{c,3}$ as it is assumed that the cake need some time to compress. Therefore, the values of $R_{c,2}$ and $R_{c,5}$ are chosen as the cake resistance 15 s after a change in pressure. From this approach, α_0 and P_a values can be estimated properly prior to the fitting process.

Approach B

An alternative approach for obtaining reliable fits of J_{LIM}, α_0 and Pa is to fit:

- J_{LIM} covering the entire span of the TMP step experiment, and
- α for each individual pressure

by the RMSE method. With this approach, specific cake resistances for each TMP are obtained, illustrated in Figure 7.5.

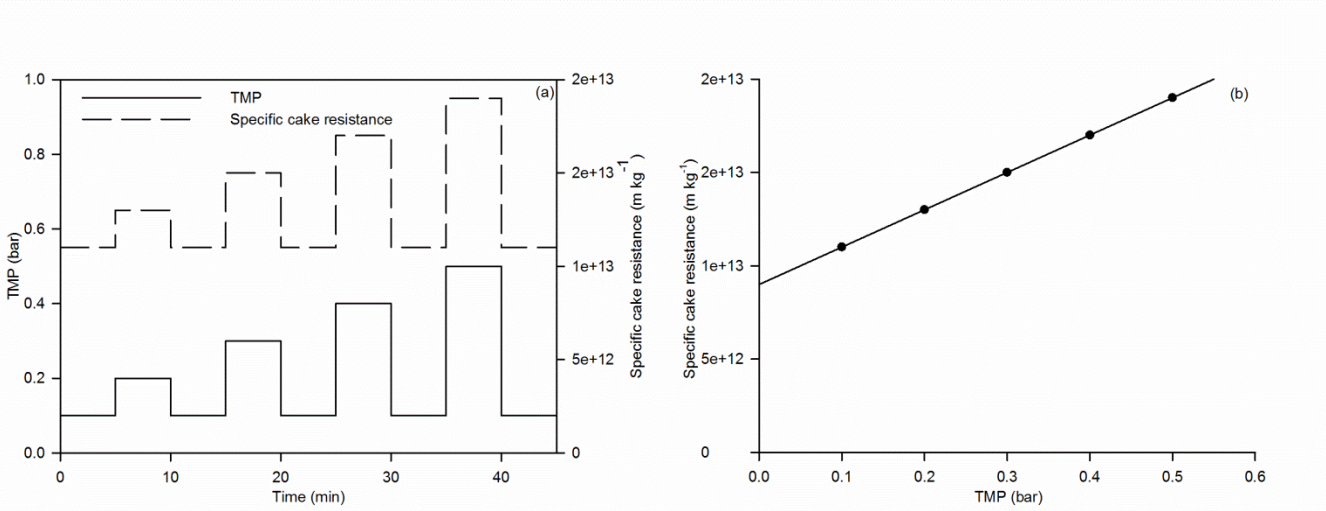

Figure 7.5: Applied TMP and proposed specific cake resistance at each step in a TMP step experiments (a) and specific cake resistance pressure dependency (b) with a regression line $\alpha = \alpha_0 + \mathrm{TMP}\cdot\alpha_0/P_a$.

From the proposed specific cake resistance pressure dependency α_0 and P_a can be determined with a linear regression according to Eq. 6.1. These parameters are valid constant for the entire TMP step experiments. This method does not rely on assumption of a constant amount of cake before and after pressure changes, as in Approach A, and is more straightforward. However, it is only possible to use, if the pressure applied to the cake is constant for each TMP step, hence $\Delta P_c = TMP$. Therefore, it is possible to use this approach for the data in Paper V, where the pressure applied to the cake is constant as the resistance of the membrane is negligible to the resistance of the cake layer.

7.2 Critical flux and back transport

In Paper I, results from TMP step experiments at different rotation speeds of the membrane discs were analyzed with the critical flux concept. This showed that there was a critical flux above which, foulants were deposited on the membrane. The critical flux depended on the rotation speed, due to enhanced back transport of foulants, in correlation with increasing shear giving higher critical flux observed by Defrance and Jaffrin (1999a). Below this critical flux, there was a straight line correlation between flux and TMP, as no deposition occurred, i.e. there was a constant filtration resistance. However, the filtration resistance was higher than the membrane resistance giving a lower flux. This has also been observed in other MBR studies and explained by adsorption and concentration polarization [Field et al., 1995; Bacchin et al., 2006].

In Paper II it is found that the critical flux occurs as the critical deposit concentration is reached, as illustrated in Figure 7.6. This is found by modeling the steady state flux after 1 hr of filtration at varying TMP with the

approach presented in 7.1 and using the cake dependent back transport function, Eq. 5.3. The figure also shows the membrane resistance and the development in cake resistance modeled over time.

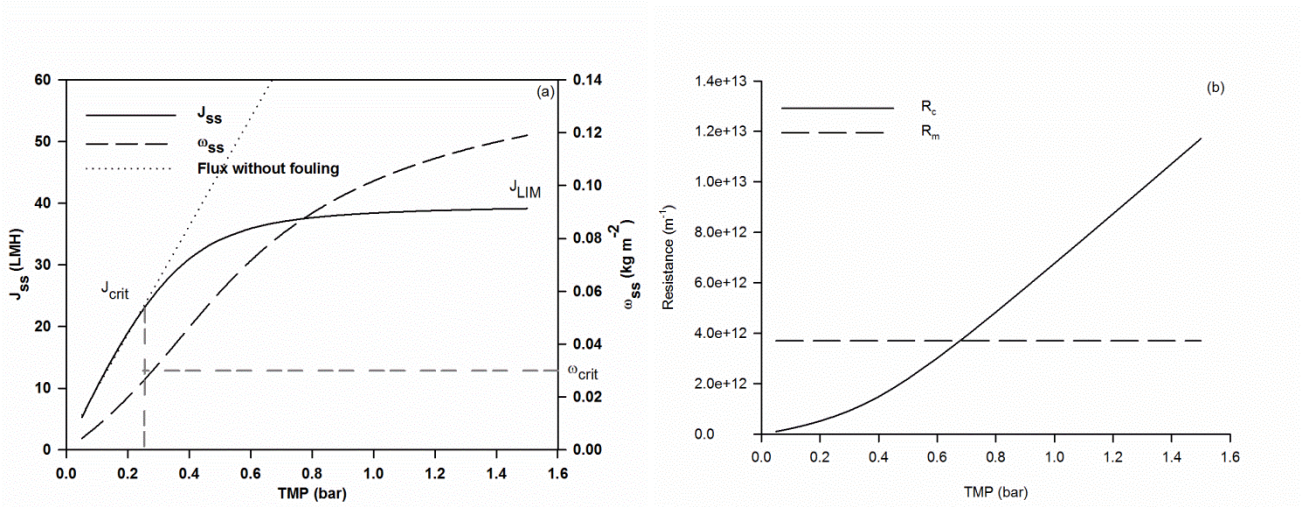

Figure 7.6: Modeled steady state fluxes at varying TMP and amount of cake at steady state. From Paper II.

This shows that when a sufficient amount of cake has formed, ω_{crit}, the steady state flux is no longer linear with TMP, hence the critical flux is reached. Above this amount of cake, the steady state flux starts to become independent of TMP and levels of at J_{LIM}. The cake resistance increases with TMP as a result of the higher amount of cake deposited and a higher specific cake resistance.

If the back transport was independent of the amount of deposited material, the steady state flux versus TMP curve in Figure 7.6a would have increased linearly with TMP until J_{LIM} is reached and the steady state flux would be constant with TMP. Hence, a critical flux for fouling cannot be observed without describing the back transport as a function of amount of deposited material as in Eq. 5.3. It is worth noting, that the relationship between critical flux and limiting flux is $J_{crit} = 2/3\ J_{LIM}$, which is also found by Bacchin (2004).

7.3 Perspectives of modeling

The modeling approach presented combined with the TMP step experimental procedure opens up for a method for characterization of fouling in membrane bioreactors under varying operating parameters. The output of the process of fitting modeled data to experimental data from a stepping experiment is J_{LIM}, describing the back transport of foulants, and α_0 and P_a, describing the fouling layers filtration properties. This approach can be used as a tool for:

- Characterization of fouling propensity respective to sludge characteristics, filtration module and operational conditions
- Simulate process to minimize energy consumption
- Designing filtrations by simulations

J_{LIM} depends on the filtration module geometry, shear and sludge characteristics, while α_0 and P_a are linked to sludge characteristics and to some extent the shear level during formation of the fouling layer. Hence, by performing TMP step experiments followed by fitting the model to experimental data, information about the filtration properties of the sludge at given operational conditions are given.

Monitoring filtration data for a given plant over time with this approach will suggest if changes of filtration properties are caused by insufficient back transport/removal of cake (J_{LIM}), high resistance of the fouling layer (α_0), a highly compressible structure (P_a) or if R_M has developed. This has been done in a study related to this Ph.D. study on a pilot scale MBR installed at Lundtofte municipal WWTP [Bugge et al., 2012]. Thereby, operators can improve filtration properties by either:

1. Enhancing shear (higher J_{LIM}) or intensification of physical cleaning
2. Change sludge cake filtration properties (α_0 and P_a) e.g. by addition of fine particles [Teychene et al., 2011] or by flocculation of sludge [Van den Broeck et al., 2010].
3. Reduce membrane resistance/background resistance by removing irremovable/irreversible fouling with chemical cleaning

Grundfos BioBooster A/S is currently investigating if this approach can be used to control filtration processes.

With the information obtained from modeling flux data from a TMP step protocol, Bugge et al. (2013) has proposed a procedure for determination of sludge specific fouling propensity. This method combines the presented TMP step modeling approach with a mobile membrane that is immersed into MBR sludge, inspired by established methods such as DFCm, BFM and MBR-VFM.

The model can potentially also be utilized to determine the effect of shear by e.g. membrane rotation speed. Performing TMP step experiments at different rotation speeds of membrane discs during filtration of sludge with given characteristics, will give a distribution of J_{LIM} vs. rotation speed that can be fitted to Eq. (5.11). Using α_0 and P_a from the same TMP step experiments, the development in flux at different rotation speeds can be simulated by use of the combined cake buildup and compression model. By comparing the production rate of permeate at different rotation speeds to the energy consumption for membrane rotation in sludge, the rotation

speed with the lowest energy consumption per amount of produced permeate volume can be determined. In this way, the filtration process can be designed to be more energy efficient. This approach is currently being investigated by Grundfos BioBooster A/S as a procedure for minimizing energy consumption of MBR systems.

In its present form, the model assumes homogenous development of fouling over the membrane. Although Paper III has shown the distribution of fluxes over membranes due to differences in shear, the "averaged" values seems to represent filtration characteristics well. However, by use of e.g. computational fluid dynamics (CFD) studies the distribution of fouling over the membranes should be accounted for, for developing the model further.

For characterization and simulation of filtrations over longer time, the model should be further developed to describe the formation of irreversible fouling and removal efficiency by physical cleaning, i.e. relaxation and backwash. The model has already been shown to be able to simulate the removal of fouling during relaxation phases, but it should be studied how relaxation time and backwash parameters influences the removal of fouling.

A model for the flux as function of reversible cake formation and irreversible fouling can have the form:

$$J = \frac{TMP}{\mu(R_m + \alpha \cdot \omega_c + R_i)} \qquad (7.5)$$

$\alpha \cdot \omega_c$ is the cake resistance and R_i is the development of irreversible fouling, which is a function of time, EPS concentration, etc. Two papers, where the development in fouling over time is modeled, have already been published [Robles et al., 2013a; Robles et al., 2013b]. The studies adopted the modeling approach for cake buildup and compression from Paper I and IV, and developed the model to describe the development of irreversible fouling in a submerged anaerobic MBR.

8. Online monitoring of membrane fouling

8.1 Methods to monitor membrane fouling

The on-line characterization of fouling in membrane bioreactors has so far focused on interpretations of flux and TMP data by stepping experiments [Le-Clech et al., 2003; van der Marel et al., 2009], modeling [Giraldo and LeChevallier, 2006; Ho and Zydney, 2006; Li and Wang, 2006], and analysis of the rate of permeability loss [Monclus et al., 2011]. Changes in fouling resistance can, as shown in this thesis, either be a result of a change in amount of fouling or changes in and specific resistance of the fouling layer. These can be difficult to distinguish between. Therefore, there is a potential for a more qualitative characterization of fouling layers by use of fouling monitoring techniques.

Post-mortem analysis has already been applied to characterize fouling layers after filtration, e.g. by confocal laser scanning microcopy (CLSM) [Juang et al., 2010; Sun et al. 2011]. However, as shown in Chapter 5, the developed cake is easily removable as filtration is stopped. Therefore, it is unclear whether it is the actual cake being examined during these post-mortem analyses, or if the cake characteristics found from post-mortem analysis represents the cake characteristics during filtration.

The demand for in-situ, non-invasive and real-time monitoring of fouling layers have resulted in an increasing number of studies that describe the development of techniques that can monitor fouling [Chen et al., 2004]. These methods are grouped into optical and non-optical techniques.

Optical techniques for monitoring membrane fouling on-line include direct observation through membrane (DOTM) and laser triangulometry. The principle of DOTM is use of an optical microscope to detect the fouling layer through a transparent membrane. With laser triangulometry, a laser light is shone through the feed side of a filtration module directly towards the membrane. A growing fouling layer gives another reflection than the reflection of the clean membrane. Therefore, from the change in angle of measurement of the reflected beam, the cake layer height can be determined during filtration of e.g. diatomaceous earth suspensions [Altmann and Ripperger, 1997]. Furthermore, Laser sheet at grazing incidence (LSGI) has been used in a study by Loulergue et al. (2011) to study fouling of melamine particles together with ultrasonic time domain reflectometry (UTDR).

The optical methods for fouling monitoring have a common limitation; they cannot visualize fouling in a turbid feed stream system, as they need an optical window [Chen et al., 2004]. Hence, to monitor fouling of membranes in MBRs on-line, another approach is needed. Of the non-optical techniques, impedance spectroscopy and ultrasonic reflectometry (UR) are the most widespread. Impedance spectroscopy uses alternating currents at

varying frequencies and amplitudes to determine the capacitance and resistance of the membrane. These change as the membrane is fouled. However, impedance spectroscopy is limited by the high impedance of polymeric membranes, making it difficult to analyze fouling on polymeric membranes.

Ultrasonic reflectometry is a non-invasive, real-time and on-line technique that was used for monitoring membrane fouling for the first time by Mairal et al. (1999). The method has since then been shown to be able to monitor membrane fouling in a wide range of membrane processes and is not significantly affected by the turbidity of the feed stream.

One way of using ultrasonic technology for fouling monitoring is to determine the thickness of fouling layers via UTDR. When an ultrasonic wave sent from an ultrasonic transducer encounters an interface a wave is reflected due to the energy partition between the surfaces. From the difference in arrival time of the reflected ultrasonic wave from the fouling layer and the membrane the height of the fouling layer can be determined. With this principle, fouling layer thickness has been measured during filtration of paper mill effluent [Li et al., 2002], kaolin particles [Li and Sanderson, 2002] and colloidal silica [Sim et al., 2012].

The individual reflection peaks for the feed/fouling layer interface and the fouling layer/membrane interface will only occur if the fouling layer has different ultrasonic properties than the membrane, which is the case in filtration of the aforementioned inorganic foulants. However, the ultrasonic properties of the organic- and biofouling layers are similar to those of the water-swollen membrane which limits the formation of a separate reflection peak from the fouling layer. A solution to this has been proposed by Sim et al. (2013) by adding a colloidal silica ultrasonic enhancer to a bacterial feed suspension in order to detect an ultrasonic peak from the biofouling layer.

Alternative to quantifying fouling from a change in arrival time of a reflected fouling layer peak, other studies have used ultrasonic reflectometry (UR) to detect fouling by the change in amplitude of the membrane reflected wave when the membrane is fouled. This has been done for inorganic fouling as well as organic and biofouling. In a study of calcium sulfate scaling of a reverse osmosis (RO) membranes the onset of fouling was detected as a reduction in membrane amplitude [Lu et al., 2012]. UR studies of pore blocking revealed increasing amplitude with the degree of protein fouling [Kujundzic et al., 2010]. Also biofilm formation has been detected with ultrasonic reflectometry, where the formation of a layer on the membrane reduced the total reflected power from the membrane [Kujundzic et al., 2007]. Furthermore, UR has been used to monitor fouling of yeast suspensions, brown surface waters and oily sludge [Sikder et al., 2006; Xu et al., 2009; Li et al., 2012b].

8.2 Ultrasonic reflectometry to monitor sludge fouling

As UR is a technique that without an optical window can monitor inorganic, organic and biofouling of membranes in different membrane systems, a method to monitor and characterize activated sludge fouling with UR was developed and described in Paper VI.

In the study, diluted sludge was used in order to be able to link the early-stage formation of fouling layers to changes in ultrasonic amplitude. The procedure used two ultrasonic transducers, to record the ultrasonic spectra of the waves reflected up- and downstream on the MF polymeric membrane (0.2 µm average pore diameter). Prior to fouling, the membrane was compacted by filtration of water to establish a baseline for the relative membrane amplitude. After this, diluted activated sludge was filtrated in time series experiments of 15, 30 and 60 min to form varying degrees of sludge fouling. As sludge was introduced, the flux declined due to fouling, while the amplitude of the membrane reflected wave was reduced as a result of the cake layer serving as an impedance matching layer to the water swollen membrane.

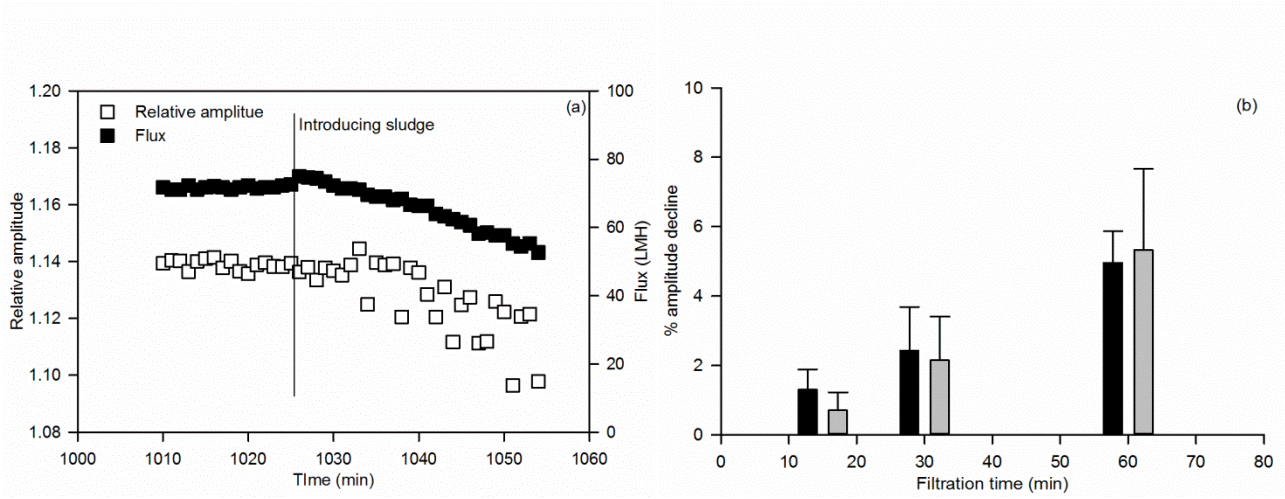

Figure 8.1: (a) Development in flux and relative amplitude before and after introducing sludge (a) in ultrasonic reflectometry studies of membrane fouling and (b) amplitude reduction vs. filtration time for upstream transducer (black) and downstream transducer (gray).

The time series experiments show increasing amplitude reduction with increasing filtration time and, accordingly, post-mortem gravimetric membrane analysis showed more fouling present at longer filtration times and, hence, amplitude reductions.

Furthermore, membranes were fouled over 5 h at pressures of 0.15 bar and 0.25 bar, respectively, to study the influence of pressure on the amplitude of the reflected ultrasonic wave. The normalized amplitude reductions are plotted in Figure 8.2.

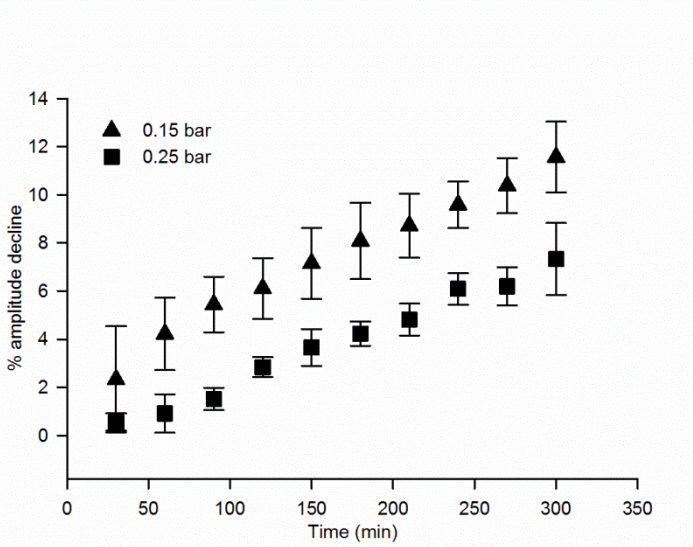

Figure 8.2: Development in amplitude reduction of membrane reflected wave over time for diluted activated sludge filtration at TMP of 0.15 bar and 0.25 bar.

The results from the experiments at different pressures show increasing amplitude reduction with time as the membrane is fouled. Furthermore, the results show that the reduction of amplitude is lower at higher pressures, although the fouling resistance is higher at higher pressures. This observation can be explained by viscoelastic properties of the cake layer. At lower pressures, more porous cakes and water swollen cake layers are formed. These will match the impedance matching of a water swollen membrane more than a compressed and dense layer will therefore give a lower reflection of an ultrasonic wave. This confirms the effect of sludge cake layer compressibility described in Chapter 6. Alternatively, it can be explained from more ultrasonic signal being perplexed as it travels through a thick and loose structure than if it travels through a thinner and denser structure obtained at a higher pressure.

The trend of higher membrane amplitude reductions observed at lower pressures was also observed in pressure step experiments. Here, the levels of amplitude reduction changed with the pressure, and did to some degree show a reversible behavior of cake resistance and amplitude reduction, when alternating between 0.15 bar and 0.25 bar TMP.

Hereby, it is shown that UR can be used as a tool to monitor and characterize sludge fouling on membranes and distinguish between sludge cake buildup and compression. In order for the UR method to be able to monitor membrane fouling in membrane bioreactors, the method has to be further developed to monitor fouling at higher sludge concentration. Special attention shall be given to the sensitivity of the amplitude reduction as a measure of degree of fouling, as higher amplitude reductions will be observed when fouling membranes with e.g. 8 g/L

sludge than 0.2 g/L sludge, as the amplitude reduction potentially will be saturated at high amounts of fouling. Furthermore, the response of the amplitude of the membrane reflected wave is expected to be different from that of cake layer formation, as other kinds of fouling occurs, e.g. gel formation.

9. Conclusion

The main findings of the present study are:

- Short term fouling in MBRs can be described as a combined effect of cake buildup and compression
- The kinetics of cake buildup can be described by the limiting flux, which depends on operational conditions such as shear and concentration
- The cake layer is compressible and shows some degree of reversibility
- Fouling can be simulated by a simple model combining cake buildup and compression
- The fouling by activated sludge can be monitored and characterized with ultrasonic reflectometry

During short term filtration experiments with the TMP step approach the development of fouling layers was studied at different operational conditions. These experiments showed that the mass balance for development of cake determines the level of fluxes. Increasing pressure or lowering permeability of the membrane does not improve filtration, as it is the balance between flux and back transport governed by operational conditions such as shear and concentration, that controls the cake formation and thereby the level of flux.

The compressibility of cake layers was observed through TMP-step experiments, where the cake resistance jumps when increasing pressure and drops after releasing pressure. Also, as the cake resistance drops after lowering pressure, the cake swells back after being compressed, hence compression seems to be somewhat reversible.

A procedure was developed based on TMP step experiments followed by fitting a model describing flux development as a function of cake buildup and compression. The buildup and removal of cake can be described from the mass balance between the permeation drag transporting foulants towards the membrane and back transport of foulants represented by the limiting flux. The compression can be described with a pressure dependent specific cake resistance. The product of the amount of cake and specific cake resistance can then be used to calculate the cake resistance and simulate the development in flux in TMP step experiments, and the development in TMP at constant flux experiments. This model is able to give precise simulations of the experimental fluxes over a broad range of pressures with three pressure independent parameters; J_{LIM} depending in the effect of back transport from e.g. shear, and cake parameters α_0 and P_a.

The mass balance has the function that at flux levels higher than the limiting flux, the flux declines over time due to cake formation. At flux levels lower than the limiting flux the flux increases over time due to cake removal, as long as the driving forces are sufficiently high. This is seen when lowering pressure just after fouling the

membrane at a higher pressure, or when increasing shear, hence back transport, after a steady state in flux has been obtained. Therefore, the model is able to simulate not only the buildup of cake, but also the removal of cake in shear stepping experiments and relaxation phases. This shows, that the kinetics for cake buildup and removal are similar, and that the cake buildup in short term experiments is reversible. The next step for the development of the model to describe MBR fouling is to extent it to also account for the irreversible fouling by e.g. gel formation.

The combined experimental and modeling approach developed is a new way to characterize fouling propensity of different sludge conditions in different plants with varying operational conditions. The advantage of this method, is, that the output is parameters describing not only the kinetics of cake layer formation but also the filtration properties of the cake layers, hence the sludge filtration properties. Therefore, using this method as an alternative tool to the already established methods (DFCm, BFM, MBR-VFM) operators will obtain information about the influence of cake buildup, cake compression or development of residual resistance. Therefore, monitoring the development of these, the operator can decide if increasing shear (reducing cake formation) changing sludge properties (to reduce cake resistance) or apply chemical cleaning (to remove additional fouling) will have the highest impact on filtration performance.

Determining the influence of operational parameters on the formation of cake layers by the combined experimental and modeling approach developed in this study, the filtration performance can be modeled as a function of operational conditions. This can be used as a tool to minimize energy consumption by simulating the produced amount of permeate at different operational conditions and comparing this to the costs for e.g. creating shear. Hence, the operational conditions with the lowest energy consumption in terms of energy per produced volume of permeate can be estimated.

Last, it is shown that ultrasonic reflectometry can be used as a tool to detect and characterize sludge fouling layers on membranes. Results from this study confirmed the viscoelastic behavior of the sludge fouling layers formed on membranes. Ultrasonic reflectometry can. Before it can be used as a tool to monitor fouling on a MBR membrane on-line, the technology has to be further developed to detect the large cake layers formed when filtrating un-diluted activated sludge. Alternatively, it can monitor the residual fouling present on the membranes after a cleaning phase in the filtration. In this way, UR can extent the knowledge obtained from the model to monitor the irremovable/irreversible fouling.

Nomenclature

Roman letters

a	Slope of linear regression
A	Empirical filtration constant ($kg^{0.5} \cdot m^{0.5} \cdot s^{-1}$)
b	Intercept coefficient
B	Empirical exponent for shear stress
d_p	Particle Diameter (m)
CST	Capillary suction time (s)
D	Diffusion coefficient
D_S	Shear induced diffusion coefficient
D_B	Brownian diffusion coefficient
J	Permeate flux (LMH, $m \cdot s^{-1}$)
J_{BT}	Back transport flux (LMH, $m \cdot s^{-1}$)
J_c	Critical flux (LMH, $m \cdot s^{-1}$)
$J_{c,i}$	Critical flux for irreversible fouling (LMH, $m \cdot s^{-1}$)
J_{LIM}	Limiting flux (LMH, $m \cdot s^{-1}$)
J_{SS}	Steady state flux(LMH, $m \cdot s^{-1}$)
k	Velocity factor
k_a	Constant for kinetics of compression (s^{-1})
k_B	Boltzmann constant (m^2 kg s^{-2} K^{-1})
m	Fluid consistency index
n	Flow behavior index
$p(\zeta)$	Term for migration due to surface interactions between surfaces of membrane and foulants
P_a	Characteristic pressure (Pa)
P_c	Cake pressure (Pa)
$q(\tau)$	Term for migration by local hydrodynamics
r	Radius (m)
r_i	Inner radius (m)
r_o	Outer radius (m)
R^2	Coefficient of determination

R_c	Cake resistance (m^{-1})
R_f	Fouling resistance (m^{-1})
R_g	Gel layer reistance (m^{-1})
R_i	Irreversible fouling resistance (m^{-1})
R_m	Membrane resistance (m^{-1})
R_p	Pore blovking resistance (m^{-1})
t	Time (s)
T	Temperature (K, ºC)
TMP	Transmembrane pressure (bar, Pa)
TSS	Total suspended solids (kg m^{-3})
u^*	Superficial air velocity ($m \cdot s^{-1}$)
x	Axial coordinate (m)

Greek letters

α	Specific cake resistance ($m \cdot kg^{-1}$)
α_0	Specific cake resistance at no pressure ($m \cdot kg^{-1}$)
β	Empirical constant
$\dot{\gamma}_m$	Shear rate on membrane (s^{-1})
δ	Boundary layer thickness (m)
ζ	Zeta potential (mV)
μ	Dynamic viscosity of water (Pa·s)
μ_a	Apparent viscosity (mPa·s)
υ	Kinematic viscosity ($m^2 \cdot s^{-1}$)
ρ_s	Sludge density (kg m^{-3})
τ_m	Shear stress on membrane (Pa)
φ	Geometric hindrance factor
ϕ	Volume fraction of foulants
ϕ_b	Volume fraction of foulants in bulk
ϕ_w	Volume fraction of foulants at wall / membrane
$\phi_{w,max}$	Maximum volume fraction of foulants at wall / membrane

ω	Amount of fouling per membrane area ($kg \cdot m^{-2}$)
ω_c	Amount of cake per membrane area ($kg \cdot m^{-2}$)
ω_{crit}	Critical amount of fouling per membrane area ($kg \cdot m^{-2}$)
ω_{ss}	Amount of cake at steady state ($kg \cdot m^{-2}$)
Ω	Rotation speed (rpm, $rad \cdot s^{-1}$)

References

Altmann, J., Ripperger, S., 1997. Particle deposition and layer formation at the crossflow microfiltration. J. Membr. Sci. 124, 119-128.

Bacchin, P., 2004. A possible link between critical and limiting flux for colloidal systems: consideration of critical deposit formation along a membrane. J. Membr. Sci. 228, 237–241.

Bacchin, P., Aimar, P., Field, R.W., 2006. Critical and sustainable fluxes: theory, experiments and applications. J. Membr. Sci. 281, 42–69.

Bae, T.-H., Tak, T.-M., 2005. Interpretation of fouling characteristics of ultrafiltration membranes during the filtration of membrane bioreactor mixed liquor. J. Membr. Sci. 264, 151-160.

Belfort, G., Davis, R.H., Zydney, A.L., 1994. The behavior of suspensions and macromolecular solutions in crossflow microfiltration. *J. Membr. Sci.* 96, 1-58.

Bouzerar, R., Ding, L., Jaffrin, M., 2000. Local permeate flux-shear-pressure relationships in a rotating disk microfiltration module: implications for global performance. *J. Membr. Sci*. 170, 127-141.

Böhm, L., Drews, A., Prieske, H., Bérubé, P. R., Kraume, M., 2012. The importance of fluid dynamics for MBR fouling mitigation. Bioresour. Technol. 122, 50-61

Bugge, T.V., Christensen, M.L., Enevoldsen, A.D., Jørgensen, P.E., Bengtsson, J., Heinen, N., Keiding, K., 2012. Compressibility of membrane bioreactor sludge: modelling cake build-up and specific cake resistance. Conference Proceedings, World Filtration Congress, Graz, Austria.

Bugge, T.V., Christensen, M.L., Keiding, K., 2011. Studies of MLSS impact on fouling propensity in a Membrane Bioreactor using TMP steps with relaxation. Book of Abstracts, ICOM 2011, Amsterdam.

Bugge, T.V., Larsen, P., Christensen M.L., 2013. A new method combining a TMP step protocol with a fouling model for on-site determination of fouling propensity and reversibility of MBR sludge. *In Prep.*

Chen, V., Li, H., Fane, A.G., 2004. Non-invasive observation of synthetic membrane processes – a review of methods. J. Membr. Sci. 241, 23-44.

Christensen, M.L., 2006. The Effect of Filter Cake Viscoelasticity on Filtration: a Study of Activated Sludge Dewatering. PhD thesis. Aalborg University, Department of Biotechnology, Chemistry and Environmental Engineering, Aalborg, Denmark.

Christensen, M.L., Keiding, K., 2007. Creep effects in activated sludge filter cakes. Powder Technol. 177, p. 23-33.

Christensen, M.L., Nielsen, T.B., Andersen, M.B.O., Keiding, K., 2009. Effect of water-swollen organic materials on crossflow filtration performance. J. Membr. Sci. 333, 94–99.

Davis, R.H., Sherwood, J.D., 1990. A Similarity Solution for Steady-State Crossflow Microfiltration. *Chem. Eng. Sci*. 45, 3203-3209.

De la Torre, T., Iversen, V., Moreau, A. Stüber, J., 2009. Filtration Characterization methods in MBR systems: A practical comparison. Desal. And Water Treat. 9, 15-21.

De la Torre, T., Mottschall, M., Lesjean, B., Drews, A., Iheanaetu, A., Kraume, M., 2010. Filterability assessment in membrane bioreactors using an in-situ filtration test cell. Water Sci. Technol. 61, 2809- 2816.

Defrance, L., Jaffrin, M.Y., 1999a. Comparison between filtrations at fixed transmembrane pressure and fixed permeate flux: application to a membrane bioreactor used for wastewater treatment. J. Membr. Sci. 152, 203-210.

Defrance, L., Jaffrin, M.Y., 1999b. Reversibility of fouling formed in activated sludge filtration. J. Membr. Sci. 157, 73–84.

Drews, A., 2010. Membrane fouling in membrane bioreactors – Characterisation, contradictions, cause and cures. J. Membr. Sci. 363, 1-28

Espinasse, B., Bacchin, P., Aimar, P., 2002. On an experimental method to measure critical flux in ultrafiltration. Desalination 146, 91–96.

Field, R.W., Wu, D., Howell, J.A., Gupta, B.B., 1995. Critical flux concept for microfiltration fouling, J. Membr. Sci. 100, 259–272.

Ghogomu, J.N., Guigui, C., Rouch, J.C., Clifton, M.J., Aptel, P., 2001. Hollow-fibre membrane module design: Comparison of different curved geometries with Dean vortices. J. Membr. Sci. 181, 71-80.

Giraldo, E., LeChevallier, M., 2006. Dynamic mathematical modeling of membrane fouling in submerged membrane bioreactors, Proceedings of the Water Environment Federation WEFTEC (2006), 4895–4913.

Giraldo, E., LeChevallier, M., 2007. Let them wear cake. Water Environ. Technol. 19, 47-51.

Ho, C.-C., Zydney, A.L., 2006. Overview of Fouling Phenomena and Modeling Approaches for Membrane Bioreactors. Sep. Sci. Technol. 41, 1231-1251.

Huismann, I.H., Trägårdh, C, 1999. Particle transport in crossflow microfiltration – I. Effects of hydrodynamics and diffusion. Chem. Eng. Sci. 54, 271-280.

Huismann, I.H., Trägårdh, G., Trägårdh, C., 1999. Particle transport in crossflow microfiltration: II. Effects of particle-particle interactions. Chem. Eng. Sci. 54, 281-289.

Huyskens, C., Brauns, E., Van Hoof, E., De Wever, H., 2008. A new method for the evaluation of the reversible and irreversible fouling propensity of MBR mixer liquor. J. Membr. Sci. 323, 185-192.

Jaffrin, M.Y., 2008. Dynamic Shear-enhanced membrane filtration: A review of rotating disks, rotating membranes and vibrating systems. J. Membr. Sci. 324, 7-25.

Jiang, T., Kennedy, M.D., van der Meer, W.G.J., Vanrolleghem, P.A., Schippers, J.C., 2003. Controlling membrane pore blocking and filter cake build-up in side-stream MBR systems. Proceedings 5th International Membrane Science & Technology Conference (IMSTEC'03). Sydney, Australia.

Juang, Y.-C., Lee, D.-J., Lai, J.-Y., 2010. Visualizing Fouling Layer in Membrane Bioreactor. Sep. Sci. Technol. 45, 962-966.

Judd, S., 2011. The MBR Book: Principles and Applications of Membrane Bioreactors for Water and Wastewater Treatment. Second edition. Oxford (2011).

Kujundzic, E., Fonseca, A.C., Evans, E.A., Peterson, M., Greenberg, A.R., Hernandez, M., 2007. Ultrasonic monitoring of early-stage biofilm growth on polymeric surfaces. J. Microbiol. Methods 68, 458-467.

Kujundzic, E., Greenberg, A.R., Fong, R., Moore, B., Kujundzic, D., Hernandez, M., 2010. Biofouling potential of industrial fermentation broth components during microfiltration. J. Membr. Sci. 349, 44-55.

Laera, G., Giordano, C., Pollice, A., Saturno, D., Mininni, G., 2007. Membrane bioreactor sludge rheology at different solid retention times. *Water Res*. 41, 4197-4203.

Larsen, P., Jørgensen, M.K., Christensen, M.L., Nielsen, P.H., 2013. Conceptual undertanding of the build-up of fouling in MBR. *Unpublished.*

Le-Clech, P., 2010. Membrane bioreactors and their uses in wastewater treatments. Appl. Microbiol. Biotechnol. 88, 1253-1260.

Le-Clech, P., Chen, V., Fane, T.A.G, 2006. Fouling in membrane bioreactors used in wastewater treatment. J Membr. Sci. 284, 17-53.

Le-Clech, P., Jefferson, B., Chang, I.S., Judd, S.J., 2003. Critical flux determination by the flux-step method in a submerged membrane bioreactor. J. Membr. Sci. 227 81–93.

Lee, C.H., Park, P.K., Lee, W.N., Hwang, B.K., Hong, S.H., Yeon, K.M., Oh, H.S., Chang, I.S., 2008. Correlation of biofouling with the bio-cake architecture in an MBR. Desalination 231, 115-123.

Lee, S.A., Fane, A.G., Amal, R., Waite, T.D., 2006. The effect of Floc Size and Structure on Specific cake Resistance in Dead-End Microfiltration. Sep. Sci. Technol. 38, 869-887.

Lee, Y., Clark, M.M., 1997. A numerical model of steady-state permeate flux during cross-flow ultrafiltration. *Desalination*. 109, 241-251.

Leighton, D.T., Acrivos, A., 1987. The shear-induced migrations of particles in concentrated suspensions. J. Fluid. Mech., 181, 415-439.

Lesjean, B., Huisjes, E.H., 2008. Survey of the European MBR market: trends and perspectives. Desalination 231, 71-81.

Li, J.X., Hallbauer-Zadorozhnaya, V.Y., Hallbauer, D.K., Sanderson, R.D., 2002. Cake-layer deposition, growth and compressibility during microfiltration measured and modeled using a noninvasive ultrasonic technique. Ind. Eng. Chem. Res. 41, 4106-4115.

Li, J.X., Sanderson, R.D., 2002. In situ measurement of particle deposition and its removal in microfiltration by ultrasonic time-domain reflectometry. Desalination 146 169-175.

Li, M., Lu, J., Heijman, B., Rietveld, L., 2012a. Effect of cake layer characteristics on fouling control in long time filtration without backwash for submerged ceramic MF membrane in surface water treatment. M.Sc. Project. Delft University of Technology, Delft, The Netherlands.

Li, X.H., Li, J.X., Wang, J., Zhang, H.W., Pan, Y.D., 2012b. In situ investigation of fouling behavior in submerged hollow fiber membrane module under sub-critical flux operation via ultrasonic time domain reflectometry. J. Membr. Sci. 411, 137-145.

Li, X.-Y., Wang, X.-M., 2006. Modeling of membrane fouling in a submerged membrane bioreactor. J. Membr. Sci. 278, 151-161.

Liang, S., Zhao, T., Zhang, J., Sun, F., Liu, C., Song, L., 2012. Determination of fouling-related critical flux in self-forming dynamic membrane bioreactors: Interference of membrane compressibility. J. Membr. Sci. 390-391, 113-120.

Lim, A.L., Bai, R., 2003. Membrane fouling and cleaning in microfiltration of activated sludge wastewater. J. Membr. Sci. 216, 279-290.

Loulergue, P., André, C., Laux, D., Ferrandis, J.-Y., Guigui, C., Cabassud, C., 2011. In-situ characterization of fouling layers: which tool for which measurement? Desal. Water Treat. 34, 156-162.

Lousada-Ferreira, M., Geilvoet, S., Moreau, A., Atasoy, E., Krzeminski, P., van Nieuwenhuijzen, A., van der Graaf, J., 2010. MLSS concentration: Still a poorly understood parameter in MBR filterability. Desalination 250, 618-622.

Lu, X.Y., Kujundzic, E., Mizrahi, G., Wang, J., Cobry, K., Peterson, M., Gilron, J., Greenberg, A., 2012. Ultrasonic sensor control of flow reversal in RO desalination - Part 1: Mitigation of calcium sulfate scaling. J. Membr Sci. 419, 20-32.

Mairal, A.P., Greenberg, A.R., Krantz, W.B., Bond, L.J., 1999. Real-time measurement of inorganic fouling of RO desalination membranes using ultrasonic time-domain reflectometry. J. Membr. Sci. 159, 185-196.

Meng, F., Chae, S.-R., Drews, A., Kraume, M., Shin, H.-S., Yang, F., 2009. Recent advances in Membrane Bioreactors: Membrane fouling and membrane material. Water Res. 43, 1489-1512.

Meng, F., Chae, S.-R., Shin, H.S., Yang, F., Zhou, Z., 2012. Recent advances in Membrane Bioreactors: Configuration Development, Pollutant Elimination, and Sludge Reduction. Environ. Eng. Sci. 29, 139-160.

Meng, F., Shi, B., Yang, F., Zhang, H., 2007. New insights into membrane fouling in submerged membrane bioreactor based on rheology and hydrodynamics concepts. J. Membr. Sci. 302, 87-94.

Moll, R., Veyret, D., Charbit, F., Moulin, P., 2007. Dean vortices applied to membrane process Part I: Experimental approach. J. Membr. Sci. 288, 307-320.

Monclus H., Ferrero, G., Buttiglieri, G., Comas, J., Rodriquez-Roda, I., 2011. Online monitoring of fouling in submerged MBRs. Desalination 277, 414-419.

Ognier, S., Wisniewski, C., Grasmick, A., 2002. Characterization and modeling of fouling in membrane bioreactors. Desalination 146, 141-147

Ognier, S., Wisniewski, C., Grasmick, A., 2004. Membrane bioreactor fouling in sub-critical conditions: a local critical flux concept. J. Membr. Sci. 229, 171-177.

Pollet S., Guigui, C., Cabassud, C., 2009. Influence of intermittent aeration and relaxation on a side-stream membrane bioreactor for municipal wastewater treatment. Desal. Water Treat. 6, 108-118.

Pollice, A., Giordano, C., Laera, G., Saturno, D., Mininni, G., 2007. Physical characteristics in a complete retention membrane bioreactor. Water Res. 41, 1832-1840.

Ratkovich, N., Bentzen, T.R., Rasmussen, M.R., 2012a. Energy consumption in terms of shear stress for two types of membrane bioreactors used for municipal wastewater treatment proceses. Arch. Thermodyn. 33, 85-106.

Ratkovich, N., Chan, C.C.V., Bentzen, T.R., Rasmussen, M.R., 2012b. Experimental and CFD simulation of wall shear stress for different impeller configurations and MBR activated sludge. Water Sci. Technol. 65, 2061-2070.

Rayess, Y.E., Albasi, C., Bacchin, P., Thaillandier, P., Mietton–Peuchot, M., Devatine, A., 2011. Cross-flow microfiltration of wine: effect of colloids on critical fouling conditions, J. Membr. Sci. 385–386, 177–186.

Ripperger, S., Altmann, J., 2002. Crossflow microfiltration – state of the art, Sep. Purif. Technol. 26, 19-31.

Robles, A., Ruano, M.V., Ribes, J., Seco, A., Ferrer, J., 2013a. A filtration model applied to submerged anaerobic MBRs (SAnMBRs). J. Membr. Sci. 444, 139-147.

Robles, A., Ruano, M.V., Ribes, J., Seco, A., Ferrer, J., 2013b. Mathematical modeling of filtration in submerged anaerobic MBRs (SAnMBRs): Long-term validation. J. Membr. Sci. 446, 303-309.

Rosenberger, S., Kubin, K., Kraume, M., 2002. Rheology of Activated Sludge in Membrane Bioreactors. Eng. Life Sci. 2, 269-275.

Shimizu, Y., Okuno, Y.-I., Uryu, K., Ohtsubo, S., Watanabe, A., 1996. Filtration characteristics of hollow fiber microfiltration membranes used in membrane bioreactors for domestic wastewater treatment. Water Res. 30, 2385-2392.

Sikder, S.K., Mbanjwa, M.B., Keuler, D.A., McLachlan, D.S., Reineke, F.J., Sanderson, R.D., 2006. Visualization of fouling during microfiltration of natural brown water by using wavelets of ultrasonic spectra. J. Membr. Sci. 271, 125-139.

Sim, S.T.V., Chong, T.H., Krantz, W.B., Fane, A.G., 2012. Monitoring of colloidal fouling and its associated metastability using ultrasonic time domain reflectometry. J. Membr. Sci. 401, 241-253.

Sim, S.T.V., Suwarno, S.R., Chong, T.H., Krantz, W.B., Fane, A.G., 2013. Monitoring membrane biofouling via ultrasonic time-domain reflectometry enhanced by silica dosing. J. Membr. Sci. 428, 24-37.

Stricot, M., Filali, A., Lesage, N., Spérandio, M., Cabassud, C., 2010. Side-stream membrane bioreactors: Influence of stress generated by hydrodynamics on floc structure, supernatant quality and fouling propensity. Water Res. 44, 2113-2124.

Sun, C., Fiksdal, L., Hanssen-Bauer, A., Rye M.B., Leiknes, T., 2011.Characterization of membrane biofouling at different operating conditions (flux) in drinking water treatment using confocal laser scanning microscopy (CLSM) and image analysis. J. Membr. Sci. 382, 194-201.

Sørensen, B.L., Sørensen, P.B., 1997a. Applying cake filtration theory on membrane filtration data. Water Res. 44, 665–670.

Sørensen, B.L., Sørensen, P.B., 1997b. Structure compression in cake filtration. J. Env. Eng. 123, 345–353.

Teychene, B., Guigui, C., Cabassud, C., 2011. Engineering of an MBR supernatant fouling layer by fine particles addition: a possible way to control cake compressibility. Wat. Res. 45, 2060–2072.

Tiller, F.M., Hayness, S., Lu, L.-M., 1972. The role of porosity in filtration VII: Effect of side wall friction in compression-permeability cells. AIChE J. 18, 13-20.

Tiller, FM, Yeh, CS, 1987. The role of porosity in filtration. Part XI: Filtration followed by expression. AIChE J. 33, 1241-1256

Tiller, F.M., Kwon, J.H., 1998. Role of porosity in filtration: XIII. Behavior of highly compactible cakes. AIChE J. 44, 2159–2167.

Van den Broeck, R., Van Dierdonck, J., Caerts, B., Bisson, I., Kregersman, B., Nijskens, P., Dotremont, C., Van Impe, J.F., Smets, I.Y., 2010. The impact of deflocculation-reflocculation on fouling in membrane bioreactors. Sep. Sci. Technol. 71, 279-284.

van der Marel, P., Zwijnenburg, A., Kemperman, A., Wessling, M., Temmink, H., van der Meer, W., 2009. An improved flux-step method to determine the critical flux and the critical flux for irreversibility in a membrane bioreactor. J. Membr. Sci. 332, 24–29.

Van Kaam, R., Anne-Archard, D., Alliet, M., Lopez, S., Albasi, C., 2006. Aeration mode, shear stress and sludge rheologyin a submerged membrane bioreactor: some keys of energy saving. Desalination 199, 482-484.

Wang, Q., Wang, Z., Wu, Z., Ma, J., Jiang, Z., 2012. Insights into membrane fouling of submerged membrane bioreactors by characterizing different fouling layers formed on membrane surfaces. Chem. Eng. J. 179, 169-177.

Wang, Z., Wu, Z., 2009. A Review of Membrane Fouling in MBRs: Characteristics and Role of Sludge Cake Formed on Membrane Surfaces. Sep. Sci. Technol. 44, 3571-3596.

Wisniewski, C., Grasmick, A., 1998. Floc size distribution in a membrane bioreactor and consequences for membrane fouling. Colloids Surf. A 138, 403-411.

Wu, B., Fane, A., 2012. Microbial relevant fouling in membrane bioreactors: Influencing factors, characterization, and fouling control. Membranes 2, 565-584

Wu, B., Kitade, T., Chong, T.H., Uemura, T.H., Fane, A.G., 2012. Role of initially formed cake layers in limiting cake fouling in membrane bioreactors. Bioresour. Technol. 118, 589-593.

Xu, X., Li, J., Xu, N., Hou, Y., Lin, J., 2009. Visualization of fouling and diffusion behaviors during hollow fiber microfiltration of oily wastewater by ultrasonic reflectometry and wavelet analysis. J. Membr. Sci. 341, 195-202.

Yamamoto, K., Hiasa, M., Mahmood, T., and Matsuo, T., 1989. Direct solid-liquid separation using hollow fiber membrane in an activated sludge aeration tank. Water Sci. Technol. 21, 43-54.

Zhang, J., Chua, H.C., Zhou J., Fane A.G., 2006. Factors affecting the membrane performance in submerged membrane bioreactors. J. Membr. Sci. 284, 54-66.

Zydney, A.L., Colton, C.K., 1986. A concentration Polarization Model for the filtrate Flux in Cross-Flow Microfiltration of Particulate Suspensions. Chem. Eng. Commun. 47, 1-21.